UNIVERSIDAD CARLOS III DE MADRID

Department of Signal Theory and Communications

DOCTORAL THESIS

STRESS LEVEL ASSESSMENT WITH NON-INTRUSIVE SENSORS

Author: FRANCISCO HERNANDO GALLEGO

Supervised by: ANTONIO ARTÉS RODRÍGUEZ

APRIL, 2018

Tesis Doctoral:	STRESS LEVEL ASSESSMENT WITH NON-INTRUSIVE SENSORS
Autor:	Francisco Hernando Gallego
Director:	D. Antonio Artés Rodríguez
Fecha:	APRIL, 2018

Tribunal

Presidente: Joaquín Míguez Arenas

Vocal: María Isabel Valera Martínez

Secretario: Luis Ignacio Santamaría Caballero

Money makes the world go round.

legal or illegal,

good guys or bad guys,

we all chase money.

This work was supported by the project 'Situational Awareness Virtual Environment (SAVIER) fellowship' from AIRBUS Group Company.

Acknowledgements

First of all, I want to express my gratitude to Antonio Artés Rodríguez for his guidance. He has supported and enabled this thesis in all possible ways and has also taught me how to become a collaborator, researcher, and human being. I also want to acknowledge Fernando Pérez Cruz, who has give me an opportunity to enroll an internship in Switzerland focusing on sport betting and learn new ways of thinking. Both will always be a role model to follow.

I would like to thank everyone in our research group, past and present: Alberto, Alex, Alfred, Aurora, David R., Deniz, Fran I, Gesús F., Gonzalo R., Gonzalo V., Icíar, Isa, Juanjo, Luca, Melanie, Pablo G., Pablo M., Pablo O., Paloma, Sara, Tobi, Víctor E. and Vivian, for making this time really enjoyable. Thanks for all the laughs and good vibes. Grace, it has been a huge pleasure to share all our experiences in the best 'cubículo'. Thanks also David Luengo and my Bachelor Degree students: Sara, Sergio and Verónica, part of this thesis is yours.

Special thanks to my hometown friends, 'Las ranas': Álvaro, Diego, Néstor, Pablo, Sevi, Ribete and Ruso, for dealing with me at my best and worst, always supporting and encouraging me. Without all of you, I would not be writing now.

I would like to thank all my friends from 'Valseca', always standing alongside me. Distinctively, Cuqui, Mónica, Maru and Pablo M. do not change ever. Pablete, you have also become a Ph.D. photoshop-maker, ¡Congrats! my right-hand man.

Joe & Nacho, thanks for day after day analyzing and discussing sport bets. And also thanks for being always supporting me. Thanks will never suffice.

The achievement of this doctoral thesis would have never been possible without the unwavering support of my family and beloved ones. Thank you to my parents and sisters, Maxi & Paco, Ana & Mat and Neli, I owe you more than I could possibly express with words.

Finally, I would like to dedicate this thesis to my gparents, Emiliana & Paco and Martina & Julián, all of you *rest in peace*, I am sure that you are proud of me.

"If you want to go fast, go alone. If you want to go far, go together."

Abstract

Stress is a feeling generated by the human body to face different challenges. This occurs by activating the nervous system and hormones. The reaction often increases the respiratory rate, blood pressure, tension in the muscles, speed up the metabolism, pupil diameter decreases, etc. All these physical changes prepare the individual to react quickly and effectively to tackle a task.

Sometimes a little stress helps to be ready to overcome some confrontation, but if stress grows more and more, can cause in a wrong decision due to the anxiety situation. Even if stress became constant, it supposes a decrease of performance and could be detrimental to health. Recognize how stress affects and when occurs has become a step in medical health industry.

The aim of this thesis is to monitor a subject while is achieving a stressful task and find a relationship between stress reactions and the performance obtained. The quantification of the physiological activations varies depending on the person, and even in the same person, it can change according to the particular situation. Past studies have used self-report questionnaires to relate stress and performance but they are obtrusive, requiring the attention of the subject. Another alternative way could be to monitor these signals as stress features and obtaining an objective value.

This thesis proposes a system acquisition to acquire signals in a non-intrusive way avoiding an array of possible artifacts or out-layers that make the signal processing difficult. The activities that can be measured in this way are the followings: heart rhythm, electrodermal and cortisol hormone.

In one hand, this thesis proposes a new feature extraction model to understand physiological electrodermal reactions. Previous methods conclude with incongruent results that are not interpretable even to differentiate between relax or stress situations in a time-line. We propose a new robust algorithm that can be used in real-time (low time computability). Besides, the results are sparse in time to obtain an easily statistical and graphical interpretation.

Additionally, this thesis presents a feature extraction method of stress reactions including signal processing methods of heart rhythm and cortisol analysis. Finally, stress features are analyzed using machine learning algorithms to extract conclusions.

Three experiments have been designed in a stress elicited environment: a) the participant is elicited stress playing a variety of neurocognitive games, b) the subject is monitored while is discussing a public talk, and c) reactions of a operator of Unmanned Aerial Vehicle (UAV) are analyzed while is simulating flight mission.

The conclusions obtained from each experiment are the followings: a) the most relevant features obtained to differentiate between relax and different classes of games. They are the sparse reactions of electrodermal activity, Heart Rate Variability (HRV) and the frequency ratio in heart rhythm. b) Secondly using only these features it can be differentiated between three states: pre-talk, talk and post-talk. Finally, c) it improves a system to capture physiological responses, analyzing and concluding in real-time a stress assessment classification.

Resumen

Estrés es un sentimiento generado por el cuerpo humano para afrontar ciertos desafíos. Esto ocurre mediante la activación del sistema nervioso y las hormonas. Esta reacción suele incrementar la frecuencia respiratoria, la presión sanguínea, pone los músculos en tensión, el metabolismo, el diámetro de la pupila disminuye, etc. Todos estos cambios físicos preparan al individuo para reaccionar de manera rápida y efectiva para completar una tarea.

A veces pequeñas dosis de estrés ayudan a estar listo para superar cualquier situación adversa, pero si el estrés aumenta más y más, puede desencadenar en una situación de ansiedad. Incluso si el estrés persiste, supone una disminución del rendimiento y podría ser perjudicial para la salud. Reconocer cómo el estrés afecta y cuándo ocurre, se ha convertido en un reto de la salud médica actual.

El objetivo de esta tesis es monitorizar a un individuo mientras realiza una tarea estresante y establecer una relación entre las reacciones al estrés y el rendimiento obtenido. Cuantificar activaciones fisiológicas varía dependiendo de la persona, e incluso en la misma persona, no siempre se muestran de manera similar. Estudios anteriores han utilizado cuestionarios de autoinforme para relacionar el estrés y el rendimiento pero son molestos, requieren la atención del sujeto y/o la escala de niveles no está normalizada. Otra forma alternativa podría ser monitorizar estas señales como características de estrés y obtener un valor objetivo.

Esta tesis propone un sistema para adquirir señales de forma no intrusiva, manteniendo la calidad y evitando una serie de posibles artefactos o valores inesperados que dificultan el procesado de señal. Las actividades que se pueden medir de esta manera son: ritmo cardíaco, voz, señal electrodérmica y la hormona cortisol.

Por un lado, esta tesis propone un nuevo modelo de extracción de características para comprender las reacciones electrodermales. Métodos anteriores concluyen en resultados incongruentes que no son interpretables incluso para diferenciar entre situaciones de estrés o relajación en una línea temporal. Además, los resultados son dispersos en tiempo para obtener fácilmente una interpretación es-

tadística y gráfica correctamente.

Adicionalmente, esta tesis presenta un método de extracción de características de reacciones de estrés que incluye métodos de procesamiento de señal de ritmo cardíaco y análisis de cortisol. Finalmente, las características de estrés se analizan utilizando algoritmos de aprendizaje automático para extraer conclusiones.

Tres experimentos han sido diseñados en un entorno de estrés provocado: a) el participante es incitado con estrés al jugar una variedad de juegos neurocognitivos, b) el sujeto es monitorizado mientras está discutiendo una charla pública, y c) las reacciones de un operador de vehículos no tripulados se analizan mientras simula la misión de vuelo.

Las conclusiones obtenidas para cada experimento son las siguientes: a) las características más relevantes obtenidas para diferenciar entre relax y diferentes clases de juegos son: reacciones dispersas de actividad electrodérmica, variabilidad cardíaca y la relación de frecuencia en el ritmo cardíaco. b) Utilizando solo estas características, se puede diferenciar entre: tiempo previo a la charla, discurso y turno de preguntas. Finalmente, c) esta tesis mejora un sistema para capturar respuestas fisiológicas, analizar y concluir en tiempo real una clasificación de evaluación de estrés en una escala de clasificación.

Contents

List of Acronyms

ANS	Autonomous Nervous System
ARMA	Autoregressive–Moving-Average Model
AWGN	Additive White Gaussian Noise
BVP	Blood Volume Presure
CDA	Continuous Decomposition Analysis
CNS	Central Nervous System
DA	Driver Area
ECG	Electro Cardiogram
ECG	Electroencephalogram
EDA	Electrodermal Activity
GSR	Galvanic Skin Response
HR	Heart Rate
HRV	Heart Rate Variability
LARS	Least Angle Regression

LASSO	Least Absolute Shrinkage and Selection Operator
LDA	Linear Discriminant Analysis
LFPC	Log Frequency Power Coefficients
LOO	Leave-One-Out
MCMC	Markov Chain Monte Carlo
MSE	Mean Square Error
NS	Nervous System
PNS	Parasympathetic Nervous System
PPG	Photoplethysmography
PS	Parasympathetic System
RMSSD	Root Mean Square of Successive Differences
RPAS	Remotely Piloted Aircraft Systems
RR	Inter-Beat
SAVIER	Situational Awareness Virtual Environment
SCL	Skin Conductance Lelvel
SCR	Skin Conductance Response
SDNN	Standard Deviation of NN Intervals
SNS	Sympathetic Nervous System
SS	Sympathetic System
SVM	Support Vector Machine
TSST	Trier Social Stress Test
UAV	Unmanned Aerial Vehicle

US	United States

1 Introduction

1.1 Motivation

Stress is an involuntary reaction that is often present in our daily life. This reaction can be interpreted as a body change from a calm state, to an excited state in order to preserve our organism [29]. While a subject feels stressed, his/her body could perceive some physiological changes such as an increase of heart beating, deeper breathing, pupil dilation, muscle tension, skin sweating and other possible factors which alters his/her physical and emotional stability. These alterations and their associated evident triggers are commune in the humans day by day [14]. Stress help tune the body to face daily threats like memory acquisition or attention [69], but if stress grows, it yields wrong decisions or a lose of performance. Furthermore, continuous stress can cause a wide range of diseases like diabetes, cardiovascular disorders or immune irregularities [4]. Stress has become one of the most studied

diseases with a cost of $300 billion per year in the United States (US), [80] is even increasing in last years, assuming an important role in medical health industry.

Stress reactions activate the Nervous System (NS) which is the responsible of the human coordination transmitting signals through different parts of the body. One part, theAutonomous Nervous System (ANS), provokes involuntary reactions which are manifested in physiological signals such as electrodermal, breathing, muscle and heart rhythm activities. Physiological reactions are activated by the Sympathetic Nervous System (SNS) which mobilizes the human body in response to stress reactions like deeper respiration, increase the pulse, tense the muscles, etc. In these situations, individuals often increase arousal, concentration, activate reflexes, and prepare the body to daily situations. Inducted stress is commonly related as short-term stress. In the other hand, the Parasympathetic Nervous System (PNS) controls SNS activations since is the responsible for the regulation of internal organs of digestion and activities that occur when the body is at resting. Stress can generate long-term diseases such as lack of motivation, continuous anxiety or breakdown states.

This thesis focus on short-term stress changes. Short-time stress can decrease productivity, it can create doubts in important decisions or lead to work accidents [68]. Yerkes-Dodson Law [105] established a relationship between arousal and performance. In Figure 1.1, performance increases with arousal when the individual feels relaxed, then reaches its maximum at the highest arousal level because the subject is involved in the task, and decreases when the individual feels in a breakdown or anxiety situation.

The current challenges consist in explaining how can short-term stress should be measured and also make a relation with performance. A great variety of approaches have been proposed to interpret the Yerkes & Dodson curve. The usual approximation is to use self-questionnaire but requires the attention of the person, but this strategy is invasive. Another way to infer the performance is measuring physiological signals hormones to extract relations about different features, but also presents high variability. Moreover, external factor , such as the noise

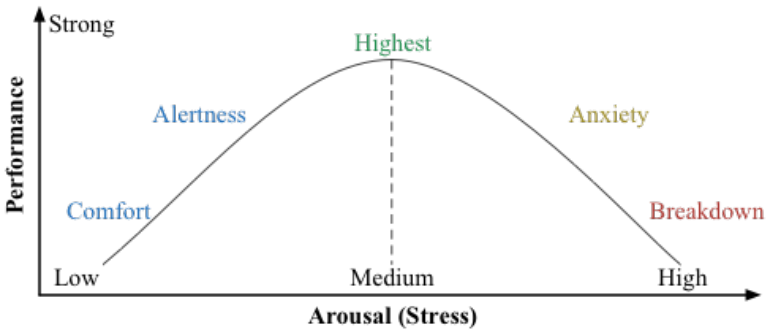

Figure 1.1: Yerkes-Dodson Law: relation between arousal and performance

perturbation, results non-interpretable.

We propose to model the relationship between stress and performance curve by the following procedure:

1. x-axis can be expressed as the arousal (in this case, the short-term stress). The x-axis represents in time, the objective stress of the subject. The individual is elicited in a controlled environment from a comfort state to an breakdown scenario,

2. and y-axis represents the performance obtained for the individual during this experiment.

Emotional states provoke changes in different physiological signals that can be measured in order to obtain information about the mental state of the individual. Among those signals, electrodermal activity varies significantly in stress situations, where skin pores start to sweat in anxiety states and the skin conductance increases due to alert situations. These symptoms can be analyze to obtain parameters of attention and short-term stress from the skin monitoring the Galvanic Skin Response (GSR). Hearth rhythm also increases blood pressure, since heart requires more oxygen to work. Two signals can be monitored: Electro Cardiogram (ECG) and Blood Volume Presure (BVP). Also other signals such as speech, hormone cortisol, Electroencephalogram (ECG) and pupil diameter can be considered biomarker patters associated with the disease stage, stress.

A wide variety of sensors can monitor these physiological signals, but: Which ones are the most effectives?. Wearable sensors are increasingly taking part in daily activities, not only because of the recent society health concern, but also due to their relevance in the medical industry. The sensor should be non-intrusive to avoid possible disturbs and also because the person who wears it could feel uncomfortable. Furthermore, the system acquisition should be designed by wireless technology. Finally, the sampling rate of the acquisition and the material of the sensor have to be revised. A large majority or sensors provide signals with artifacts and out-layers that make the difficult information extraction. The x-axis scale can be modeled using the reactions extracted from these signals.

The second problem is to fit the y-axis of the Yerkes & Dodson curve. Researchers and psychologists have recollected and analyzed stress assessment performing an approximation of self-report questionnaires. However, these emotions should be partly forced in a objective way, for example, stress elicited to the participants trying to emulate real live situations. It is needed to create a controlled environment with a experiment that generates stress and keeps the subject like s/he is performing the activity as normal. Note that the physiological signals can replace the questionnaires results avoiding any type of subjective answers.

This thesis is part of the *Situational Awareness Virtual Environment (SAVIER)* project funded by *AIRBUS Group*, whose aim is to deal the needed technology of the Remotely Piloted Aircraft Systems (RPAS) system of Unmanned Aerial Vehicle (UAV). This work is focus on the stress level assessment of the operators of UAV. The effectiveness of these operators depends on their stress level, so it would be useful to be able to monitor and evaluate this magnitude and assessment in flight missions. This project describes what stress is, from an engineering point of view, how it can be measured in non-intrusive way and analyzed for obtaining a stress level in a scale ranking.

1.2 Scientific Aims

The specific aims of the thesis are the following:

- To design a new method of electrodermal features extraction that outperforms the previous algorithms.
- To evaluate of different physiological features to know which parameters are more relevant in the stress assessment.
- To validate of the physiological features model in real-life controlled environments.
- To develop a software algorithm to automatically classify the level of stress in a five-level rating scale based on physiological reactions.

1.3 Contributions

This thesis is a multidisciplinary work, bringing an analysis to deal with real-world stress problems in the fields of public talks, individual characterization and neurocognitive games. Throughout this thesis, we introduce:

(A) A new feature extraction model of sparse electrodermal reactions.

(B) A model of the most relevant physiological features to detect stress reactions modeled in objective way using wearable sensors.

(C) A new real-time method to characterize and classify stress levels in a five-star rating scale.

The contributions of this thesis have also been or will be partially published in [37, 39, 38, 40]. This thesis provides a complete robust stress feature extraction algorithm applied to different relevant situations where stress could be controlled. We summarize our contributions in the sections below.

1.3.1 Electrodermal Feature Extraction Model

A GSR extraction technique has been developed in order to interpret Electrodermal Activity (EDA) records, which can be useful both for ambulatory and health applications. The core of the proposed approach is a feature extraction scheme

that is based on a non-negative sparse deconvolution of the observed GSR signals. Unlike previous approaches, the resulting algorithm is fast (immediately extracting the skin conductance level and response), efficient (being able to work with any sampling rate and signal length), and highly interpretable (due to the sparsity of the extracted phasic component of the GSR).

1.3.2 Stress Calibration System

This contribution presents a controlled experiment design to know which physiological features are more relevant in human decisions. During the experiments, subjects are requested to either play a neurocognitive game using a computer, or relax during interleaved intervals of time. Nine subjects performed the experiments twice and twenty four once to train the model. The main objective has been to analyze the capability of the extracted features to understand individual behaviors. A binary classification problem is proposed to determine whether a person was playing or relaxing, achieving 13.31% mean error.

1.3.3 Person-independent stress detection

This study proposes a new framework to process signals while an individual is discussing a public talk trying to classify his/her stress levels. A dataset is presented, composed of 17 one hour talks where speech, electrodermal activity and heart rhythm are recorder using non-intrusive sensors. The proposed method obtains 12 features each minute and classifies in three states: pre-presentation, talk and question time. A database of 9 presentations were used as training set and the rest of 8 talks as test data. We show that the proposed framework makes it possible to detect distinctive stress patterns, verifying an average of 15.05% percentage of error between the three classes, achieving a model to use in stress detection.

1.4 Thesis Outline

The remainder of the thesis is as follows. Chapter 2 summaries a novel state of the art of stress assessment divided in four main parts: 1) explanation of differences between long-term and short-term stress, 2) description of several approaches to measuring stress, 3) and different approaches to comfortably measure physiological signals, 4) presentation of the most important physiological signals used in stress recognition. Chapter 3 presents a new method of feature extraction for GSR signals. The model is introduced and compared with other methods developed in the past. Chapter 4 defines some feature extraction techniques for different human activities. It is divided into the description of the heart rhythm, the electrodermal activity, the speech and the hormone analysis. Chapter 5 discusses three experiment developed to elicit stress in a controlled environment and to understand the stress reactions of the participants. Finally, Chapter 6 provides some conclusions, and discuss some possible future lines.

2

Stress Assessment

This chapter describes the state-of-the-art of stress reactions. In particular, the chapter describes: 1) definition and different types of stress, 2) how the Autonomous Nervous System (ANS) reacts from stress situations, 3) objective versus subjective stress measurements, 4) a novel of the most relevant physiological signals used in stress assessment, 5) a list of possible wearable sensors, 6) and finally some experiments of stress recognition using physiological signals.

2.1 Stress Definition

Stress is a reaction that puts the body on alertness. When stress acts properly, this reaction is the best way for a subject to work under pressure. A little stress of this kind can help to remain attentive, ready to face any challenge. But stress can also cause problems when it is extreme. The response to stress could be critical in

emergency situations, such as when a driver has to stop the car suddenly to avoid an accident. It is also activated in a more simple way when the person is tense, although not in danger like when your hit can win the game; when you prepare for a public talk or when you are doing a final exam.

But stress is not always a reaction to immediate or momentary things. Progressive or long-term events, such as a divorce or moving to a new neighborhood or school, can also cause stress. Long-term situations can produce a stress of low intensity, but lasting, causing difficulties for the person. The nervous system feels a continuous tension and remains relatively active in order to continue releasing additional hormones for a prolonged period of time. This situation can deplete the body's reserves, causing the person to feel exhausted or overwhelmed, weakening the body's immune system and causing other problems.

If the body return to a relax state after a stress situation, this short-term stress reactions are transitory. Muscles should come back to a relax state, shivers disappear, etc. Highly demands and pressures in the recent years, for example at work, put the body in tension for a long period of time, continuous tiredness provoke lack of motivation, and over time, these physiological demands create fatigue problems on body.

Stress can have a critical impact on health if these symptoms make continuous and these high levels reach a maximum, such as anxiety or breakdown moments. Long-term stress can origin several diseases and affect the overalls well-being. This thesis borrows the definitions of demands in these three cases:

Short-term stress

It is body's immediate reaction to a new challenge, event, or demand, and it triggers alertness activations. It put the body in alertness until it exceeds the anxiety threshold and the body come in an breakdown situation. As the pressures of a near-miss automobile accident, an argument with a family member, or a costly mistake at work sink in, body turns on this biological response.

Long-term stress

It comes about as the result of a situation that has not been resolved or continued for many years prior to being resolved. This might be a traumatic event that happened during childhood. Although resolved, the feelings surrounding the situation may not have been dealt with and chronic stress remains. There may also be an ongoing situation, such as family abuse, dysfunctional home or an ongoing illness in the family. This stress has the ability to create additional health problems, for example heart disease or stomach ulcers.

Individual performance

Every person has different responses in presence of stress situations, but present similar behaviors performing the same activity. Performance achieved could have variance as describe [104], i.e. the time reaction for each individual carrying out a task. It is important to characterize the capacity and abilities of each person due their inter personal variability.

Measure stress levels shows a variability on how humans perceive and experience stress states. Furthermore, depending on the day, the same activity could affect different in stress even if is performed for the same person. Usual factors that influence are: whether s/he exercises frequently [69], the number of hours s/he had sleep last days [75] or the amount and type of social interactions s/he had last days [54].

2.2 Autonomous Nervous System

Nervous System (NS) can be divided in: the central division involving the brain and spinal cord and the peripheral division consisting of the autonomic and somatic nervous systems. The NS is divided into two components [78]: Central Nervous System (CNS) and ANS. This thesis will focus on the ANS, because it is the system that controls involuntary actions of the human body, such as the beating of heart, sweating or digestion. A hierarchical scheme of the NS is shown in Figure 2.1.

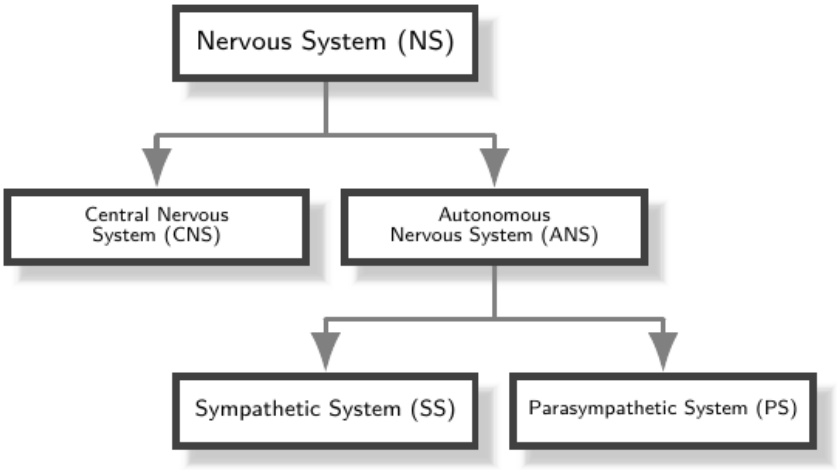

Figure 2.1: Hierarchical scheme of the Nervous System (NS).

ANS is an efferent system (i.e. it carries impulses from CNS to peripheral organs) and it can be divided into two subsystems: Sympathetic Nervous System (SNS) and Parasympathetic Nervous System (PNS). Both subsystems make actions that can seem opposite each other. The Sympathetic System (SS) acts in urgent cases causing reactions such as the fact of accelerating the pulse rhythm or the breathing or breaking the digestion. This subsystem acts on this way to prepare people in order to use their maximum energy. However, the Parasympathetic System (PS) keeps energy in order to maintain the properly operation of the human body after these urgent cases where the ANS acts.

The SS can be associated to short-term stress because carries reactions that can be measured in seconds, the short-term stress named before. In spite of, the PS responses are lingering during days or weeks, assuming the part of long-term stress.

Both subsystems control different functions of the human body which are sensitive to emotional states [77], and emotions are related to stress because people who cannot or do not know how to deal with these emotional situations are more likely to suffer stress reactions. Emotions can be elicited by perception, imagery, anticipation and action [11]. There have been several researches where different

stimuli have been applied aiming at eliciting different emotions, and it is just in this point where can take into account a set of different physiological signals that can be measured, and thus, it is possible to obtain information of the emotional state.

2.3 Objective vs Subjective Stress Analysis

The estimation of stress levels has been the focus of attention of psychologists in the past decades due to the increase of patients. Being able to automate and subsequently quantify levels of stress in daily activities can be of help to prevent the possible future manifestations of long-term stress and to understand which events cause the greatest amounts of stress [33].

Psychologist used self-report measures that can be answered at the end of the test based on retrospective experiences. Psychologists consider that these type of tests are the best way to characterize a person based on their own subjective scale of experiences. But this supposes that there is a great variety of normalizations that try to adjust the levels of stress in everyday life. For example, The Daily Stress Inventory [12] quantify the short-term stress counting the number of anxiety reactions that happen in one day. Retrospective questionnaires obtain information after the experiment but are contradictorily and affect by recall problems. These tests also requires the attention of the person, and s/he can lie because if the test is boring or too large. Besides they assume that each subject is going to answer properly and understand the question about emotions that maybe s/he does not hear never.

As the subjective measure from self-report does not have robust characteristics to be able to specify a normalized scale of stress levels, a second option is the measurement based on biological signals. Concretely, the most reliable measures are the blood tests and the hormone cortisol but the time processing is slow and it is not enough to make a precise measurement. Using bio-signals, an alternative is to process physiological signals. One example, Zimmermann et al. [108] proposed a complete system to monitor the use of the keyboard and the mouse to shows

changes relate with different state of the subject. This experiment collect lots of external and other factors and finnaly was difficult to differentiate between stress, non-stress and noise. Barreto et al. [5] in another experiment capture only physiological signals associated with stress: heart rate, pupil dilation, skin temperature and electrodermal activity, where classify in different state using a feature extraction of the named signals.

The work presented in this thesis considers the last alternative where some physiological signals are monitored. The main idea is to extract objective data to avoid possibles incongruent results in stress scales.

2.4 Stress Recognition Using Physiological Signals

The next problem is whether or not stress levels could be recognized from physiological signals using non-intrusive sensors. As was mentioned before, physiological signals are needed in order to extract information about the state of each individual. A model composed of the most relevant physiological signals used for detection stress is described below to have a reference of each one, and them, a summary of some experiments is discussed.

Galvanic Skin Response

Impulses of the sudomotor nerve used to produced and sweat glands react causing sweat diffusion when a stress situation happens. Due to this reason, skin conductance increases and transpiration can be detected by a conductivity sensor. These are the reactions of the Electrodermal Activity (EDA).

The term Galvanic Skin Response (GSR) refers to changes in the electrical properties on the surface of the skin in response to sweat secretions [9]. These secretions are due to an increment in sudomotor innervation, caused by the SNS, that results in changes in the GSR signals as the body responds to different daily circumstances: stress, temperature, anxiety, exertion situations, etc. [94]. Hence, the sympathetic activity can be measured by analyzing the GSR signals, as already shown in[53]. For instance, this relation between SNS acts and the observed

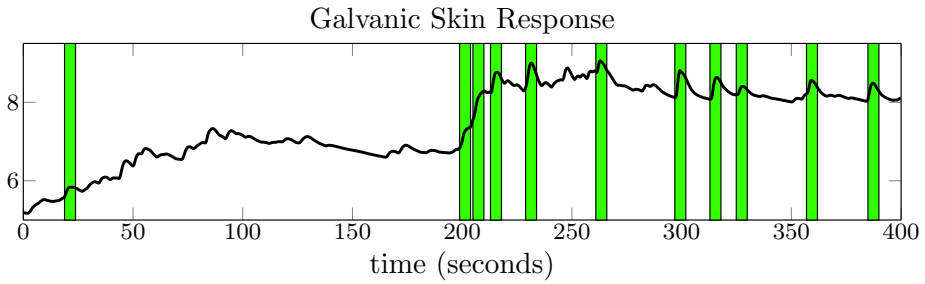

Figure 2.2: Example of Galvanic Skin Response signal of 400 seconds.

skin conductance [99], which determines the sympathetic innervation of the sweat glands [10], has been extensively used in stress detection applications (e.g., see [30, 106, 92, 31]).

GSR suffers changes in the electrical properties of a human skin due by an interaction between controlled events and the subject's state. However, there exists a big limitation in this signal. In the signal example shown in Figure 2.2, the short stress responses caused by stress are marked in green and the signal is drawn in black. In fact, this example shows that this kind of signals can be useful for stress detection if are processed correctly.

Blood Volume Pulse

In stress situations, it is known that there are changes in the number of heart beats due to the fact that pulse is increasing. Also, vasoconstrictions, i.e. contraction of the muscular wall of the vessels resulting from the narrowing of the blood vessels, increases in response to stimulus situation that can provoke stress while decreases in response to relaxation. Therefore, Blood Volume Presure (BVP) can be an useful signal to measure heart activity. One example of this signal is shwon in Figure 2.3.

This signal offers information about the heart beats and about the relative constrictions of the blood vessels. Calculate the distance between each maximum in seconds is applied in order to measure the heart rate. However, to count vaso-constrictions we have to take into account the shape of the envelope of the signal.

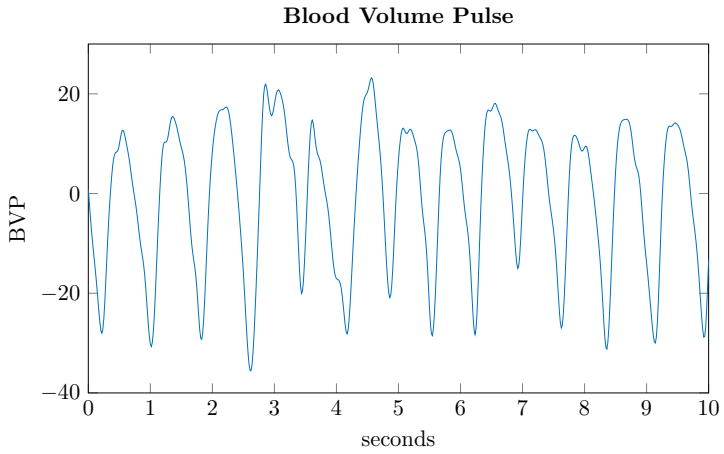

Figure 2.3: Example of a Blood Volume Pressure signal of 10 seconds.

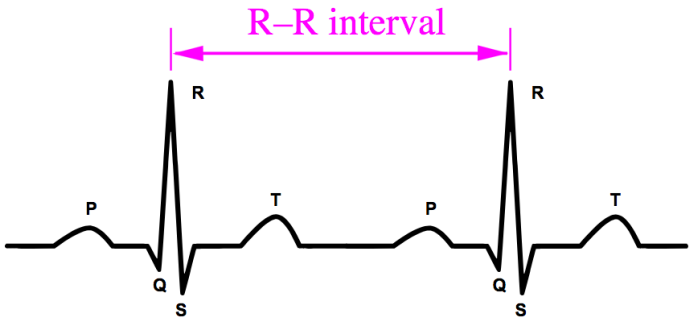

Figure 2.4: ECG signal example and RR interval definition.

Electrocardiogram

The heart activity in the cardiac system can also be measured by the Electro Cardiogram (ECG). It represents graphically the electrical activity of hearts. The electrocardiograph, that is the device which measures the ECG, is able to detect voltage on the surface of the skin when heart beats happen. An example of the signal is shown in Figure 2.4. Inter-Beat (RR) interval is defined as the time elapsed between two consecutive R waves in a electrocardiogram signal [100]. Stress also affect to compute other valuable parameter, Heart Rate Variability (HRV). Some researches, for example in [44], show that individuals who have a better stress tolerance, they could have different patterns of Heart Rate Variability (HRV) in the stress period and also before that.

Electromyogram

When the body suffers some stimulus, muscle activation reacts, which supposes an increasing in the current measured in muscles. Therefore, by measuring muscle activity we will be able to detect these current increasings corresponding to stress situation. Apparently, it can be measured in any muscle, but there are some of them that can provide more information, i. e. [73] measure the EMG on the trapeziums muscle giving good results.

As it was explained in the electrocardiogram, in order to measure these reactions that appear when a muscle is contracted we need a set of electrodes. For example in [30], they use three electrodes: two of them located along the axis of the muscle that they want to measure and the third one is the ground located out of this muscle.

As it is described, there is a significant increasing in the current measured that means that the body suffers some stimulus and muscle activation reacts.

Pupil Dilation

Pupil Dilation is wider and the eye movement is faster under a stress situation. Therefore, this is other physiological signal that can be measured in order to know the individual emotions because the ANS innervates some of the muscles that controls the pupil size.

Pupil Dilation is not used as other biosignals, such as, for instance, skin conductance, because it is more difficult to obtain the acquired signal, but there are several researches where they measured for stress detection [28] [106].

Hormone Analysis

The PS reactions, namely the long-term stress, changes the human metabolism, manifesting on the variations and concentration in hormones like cortisol. Tiredness, family problems, distractions or anxiety are examples of situations where a person's performance can decrease. [55] argues that the measure of cortisol can be an identifier pattern associated with stress as well as in terms of efficiency of

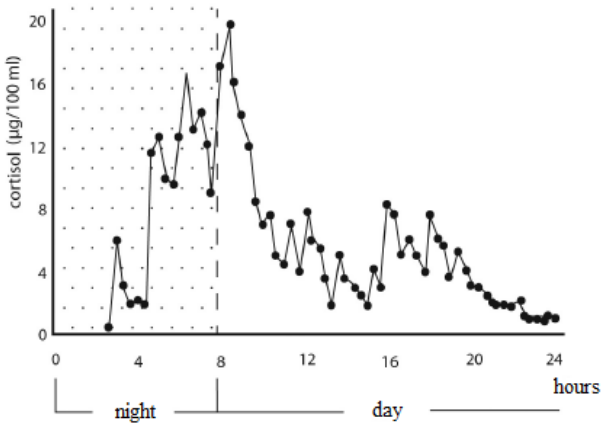

Figure 2.5: Twenty-four hour pattern of cortisol levels [102]

individual performance.

Cortisol hormone is vital for the functioning of almost every part of the body. Overabundance or deficiencies of cortisol lead to several disease states and physical symptoms. One possible application of salivary cortisol is a biochemical marker for post-traumatic psychological distress disorders and other conduct disorders [97]. Nevertheless, cortisol differs during the day with levels, as is shown in in Figure 2.5, reaches highest in the morning and lowest in the evening.

Skin Temperature

Skin temperature can change due to the sympathetic innervation of the sweat glands. The main information that can be obtained about the skin temperature is in the transient decreases when the stimulus affects to the individual. Once the acquired signal is measured, the information about when stimulus occurs due to the fact that the slope of the skin temperature signal generally shows a negative trend.

Skin Temperature is not commonly used because the signal is very noisy and can be affect for external factors. However there exist some researches where this signal is measured and used in order to extract information about it [5].

2.5 Physiological Monitoring

The development of a system composed of sensors to capture stress reactions should be non-intrusive to avoid create additional stress. The best way to capture electrocardiogram signals requires electrodes and gels attached to the skin that should be awkward especially at the time of remove it. Besides exits another factors such as keep worried with battery charging, temperature of the hormone cortisol liquid, etc. that make the acquisition more difficult. Following the example, to overcome the measurement of heart rate, the least invasive technique is the Photoplethysmography (PPG).

Wearable sensors have been recently introduced in our daily life to know how many steps we take per day, our mean heart rate or the number or the number or floors that we have gone up. Some examples: Kwon et al. [47] use the accelerometer of the mobile to extract the heart rate. Phan et al. [76] also estimates the respirotary waveform and herat rate using the accelerometer. These new methods confirms that physiological signals can be obtained in non intrusive way to model new stress models. Most of the researchers use several type of smart-wrists to know the information related to heart rhythm [33]. At the end, some many studies only use the mean heart rate to perform and statistical model so the wave of the electrocardiogram is insignificant.

This thesis evaluates how to measure heart and electrodermal activity from different smart-watches with commercially available wearable sensors. Electrodermal activity signals are more sensitive to recalled a useful signals for signals changes or artifacts. In terms of non intrusive, Shimmer [91] sensor are take placed two electrodes on the palmar surface of the middle and index finger. Another company develop two sensors: Empatica E4 [23] or Q sensor [1] which the bracelet should be placed on the wrist of the non-dominant hand. They should be wear it snugly, so that it does not move around, but not so snugly that it is uncomfortable.

The sensors used send signals via *Bluetooth* which is a technology for send and receive information over short distances. *Bluetooth* is a standard protocol designed for low-power consumption. Sensors do not need visual line of sight

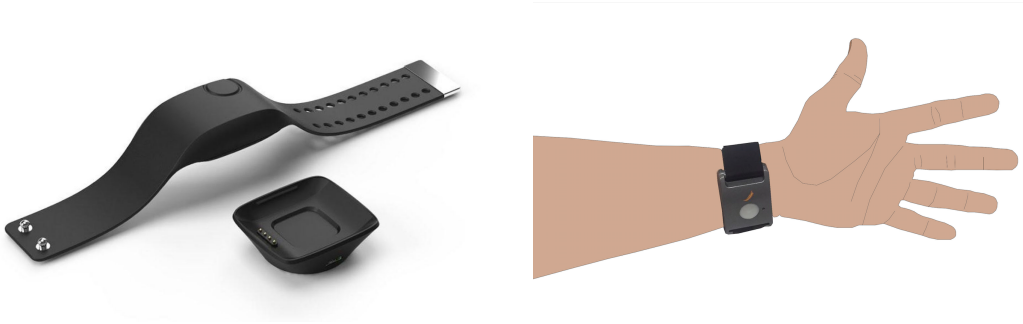

a: Empatica E4

b: Affectiva Q Sensor

Figure 2.6: Two sensor are shown: (a) Empatica E4 captures BVP and GSR signals and (b) Q sensor acquires only GSR signals.

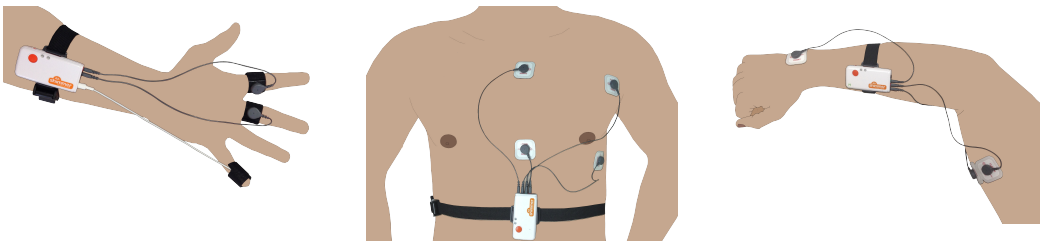

a: Shimmer used for GSR and BVP signals acquiring electrodes and optical pulse sensing probe

b: Shimmer used for the ECG measurement electrodes

c: Shimmer used for the EMG measurement electrodes

Figure 2.7: Family of Shimmer sensors is displayed.

with the receiver (in this case a computer that process the signals). This wireless protocol leave behind sensors that must need the acquisition via link because the information extracted could be also acquired via wireless without complications.

A wireless sensors list is briefly detailed below:

- Empatica E4 [23] is a compact wristband that allows obtaining data about electrodermal activity, heart rate, R-R interval, device position and angular velocity. This bracelet is shown in Figure 2.6 (a).
- Q sensor [1] allows only the measurement of galvanic skin activity through two silver electrodes placed on the base of the device. The quality obtained is better than Empatica E4. This sensor is displayed in Figure 2.6 (b).

- Speech is obtained using a Zoom H1 handheld recorder with a Rode lavalier microphone. Non lossy compressed files (wav), 24-bit quantification and 44 kHz sampling rate are used.

- A Shimmer3 'GSR Unit' sensor was used to capture BVP and GSR signals. On the left hand, the BVP optical pulse sensor was placed on the palmar surface of the pinky finger [90]. For GSR signals two electrodes on the palmar surface of the middle and index fingers were placed [89] as shown in Fig. 2.7 (a).

- Another sensor model, Shimmer3 'ExG Unit', was used to capture EMG and ECG signals. In the case of ECG, Fig. 2.7 (b) shows how the electrodes were positioned on the chest [87].

- In order to capture EMG signals, Fig. 2.7 (c) shows an example of right arm electrode layout. Two electrodes were placed in parallel with the muscle fibres of the biceps, near the centre of the muscle and the reference electrode an electrically neutral point of the body, as far away as reasonably possible from the muscle being measured [88].

- Hormone analysis is obtained from oral saliva, which is deposited in the swab shown on the right of the Figure 2.8 (a) and collected for analysis in the canister shown at the left. These devices are developed by *IproInteractive*. The swab is introduced into the canister for at least 2 minutes, mixed with the liquid being displayed within. The resulting liquid is introduced into a rectangular tank and allowed to stand exactly 10 minutes. After this period the tank is introduced in the area of testing and analysis button of the device shown in Figure 2.8 (b) is pressed. The level of cortisol is displayed in $\mu g/mL$.

a: Swab and canister.

b: Saliva tester.

Figure 2.8: Devices used for saliva analysis.

2.6 Stress Recognition In Controlled Environments

Past authors have developed different stress recognition models that can be found in the literature. The methodology to elicit stress in controlled environments is to proposed some test to the participants and collect the signals in the laboratory and scores obtained in each test. The most relevant experiment that induce stress are described below.

2.6.1 Elicit Stress Using Controlled Experiments

Stroop Color-Word Interference Test [43]

This experiment consists of a succession of words that appear on a screen with a decreasing temporal rhythm and the participant has to name the color in which the words appear. At the beginning the word coincides with the color of the word but as it progresses the time, changes to try to confuse the participant and get a Stroop effect situation.

Trier Social Stress Test (TSST) [45]

This experiment is designed to assess the vulnerability of the participant to the exposure of a speech at a social event. It has many variants, but the most common version is described below:

The approximate duration of the experiment is 15 minutes. In the first 5 minutes the participant receives a topic and has to write a scheme about the speech that will be given next. The participant will return that scheme

to the jury and during the following 5 minutes he has to present publicly what s/he has previously organized . In the case that the speech ends, s/he must expose anything else until the end of the 5 minutes. Finally, the last 5 minutes must count back from the number 1022 in step of 13. In the case of finalizing, repeat the process again until the end of the time.

Trier Mental Challenge Test (TMCT)

This test is a selection of mathematical problems. The computer screen displays the actual score un the upper left corner, the mathematical problems in the center and a horizontal bar extending from the left to the right margin on the bottom controlling the time to answers.The time allotted for problem solution varies varies with the difficulty with increasing time for more difficult problems.

After 5 minutes, the computer program stops and only the total scores are displayed. The subjects had to work on 4 trials of arithmetic problems of 5 minutes, this, the stress lasted for 20 min in total.

2.6.2 Stress Recognition from Physiological Signals

Some authors have developed a variety of techniques combining signal processing, classifications and regression methods with the purpose of make a relationship between stress and physiological signals [33]. The most relevant are described below:

Barreto, Zhai & Adjouadi [6] used the Stroop test to elicited volunteers and clustering in time stress and relax time using Support Vector Machines (SVMs). The physiological signals used were EDA, skin temperature, pupil diameter and BVP. The results confirm only a 9.90% probability of error.

Setz et al. [85] also want to differentiate between stress and cognitive load using a social evaluative test. In this case they only use EDA signals and achieve a 17.2% probability of error, using SVMs.

Shi et al. [86] wanted to discriminate between stress and relax responses under social and neurocognitive stress situations. They use SVMs and obtained 80% re-

call and 68% precision. The signals used were EDA, respiration electrocardiogram and skin temperature.

Finally, another example to comment was to Healey & Picard [29] who monitor participants during a real world driving test. They perform Linear Discriminant Analysis (LDA) in three levels: city that seems hight stress, medium (highways) and all the rest performing only a 3% of probability of error. They used the features of EDA, respiration and electromyogram of the trapezius.

3

Sparse Non-Negative Driver Model

This section presents a new method of feature extraction of Galvanic Skin Response (GSR) signals. It is divided as follows: a signal processing review of GSR methods is discussed, then, the mathematical sparse model is explained, a practical implementation of the model in 100 records is examined and finally some conclusions are considered.

3.1 Signal Processing Review For GSR signals

GSR signals carry information about Sympathetic Nervous System (SNS) activity, but are also influenced by other factors, like temperature changes or sweating due to aerobic exercise [41]. The challenge in analyzing them is thus to develop a method which is able to extract only SNS activity symptoms while avoiding other unrelated components. Indeed, GSR signals, which are usually denoted as $s(t)$,

can be expressed as a sum of two components [9]:

- The *tonic component*, $s_\ell(t)$, or Skin Conductance Lelvel (SCL), which is a slow changing signal. The SCL is related to several non-SNS activity factors but also to the level of attention of the subject, even in the absence of instantaneous stimuli.

- The *phasic component*, $s_p(t)$, also called Skin Conductance Response (SCR), which is the reaction to sporadic SNS stimuli. The SCR, which is superimposed on top of the tonic component, includes higher frequency components and appears only within specific time windows whose length typically lasts from one to five seconds [9].

Furthermore, SCRs can be modeled as the standard linear convolution between a sudomotor SNS innervation, $d_p(t)$, that corresponds to the *non-negative* unknown *sparse* driver that causes the observable skin conductance response, and the response triggered by that driver, $r(t)$. Hence, GSR signals can be finally decomposed as [49],

$$s(t) = s_p(t) + s_\ell(t) = d_p(t) * r(t) + s_\ell(t). \tag{3.1}$$

GSR signal processing models then focus on the estimation of the SCR and SCL components in the absence of other factors.

Alexander et al. [3] were the first to introduce a decomposition algorithm based on the model of Eq. (3.1). Their approach estimates first the SCL contribution, which is subtracted from $s(t)$, and then reconstructs the SCR signal using an iterative inverse filter deconvolution method. However, this method leads to a non-sparse driver that can present negative impulses, which are not physiologically interpretable. Moreover, it is very slow, thus preventing its application for long time registers or on-line signal extraction.

Benedek et al. [8] addressed the decomposition using a different signal model and considering a non-negative deconvolution scheme based on Gauss elimination to avoid negative SCRs. After estimating the SCL and subtracting it from $s(t)$,

this approach obtains an initial estimation of the SCR through a Gauss elimination deconvolution. The negative components of the SCR are then removed by introducing an arbitrary waveform that is fitted by minimizing the error with respect to the observed signal. Unfortunately, this method produces a noisy driver which is not sparse, and the waveforms introduced to force the non-negativity are not physiologically interpretable.

In another work, Benedek et al. [7] proposed an alternative non-negative decomposition based on the model of Eq. (3.1) that shows common ground with the method of [3]. It is based on a spectral division deconvolution with a Gaussian window (after removing the estimated SCL component again), and the SCR detection is performed by searching for the zeros in the first derivative of the driver. This approach yields an individual estimate of the typical SCR shape through optimization, but the estimated driver is still non-sparse and the computation is slow (as shown in the simulations).

Greco et al. [27] proposed a non-negative sparse deconvolution based on cubic B-splines for the SCR component, an Autoregressive–Moving-Average Model (ARMA) model for the sudomotor SNS innervation, and an additive white Gaussian noise term. Although the resulting convex optimization problem can be solved, the solution obtained is still not sparse (values close to zero, but not exactly equal to zero, are obtained) and the interpretability is not improved w.r.t. previous approaches. They introduce the joint estimation of the SCL and SCR components, but this method is still not fast enough for on-line application. Another sparse deconvolution technique has been introduced very recently in [42]. This approach recovers a truly sparse driver and takes into account potential discontinuities in the SCL due to motion artifacts. However, they assume that the length and shape of the response $r(t)$ are known, they do not enforce the separation between SCR events that typically occurs due to physiological reasons, and the resulting algorithm is not directly applicable for on-line extraction of SNS information.

In summary, the sparse nature of the driver $d_p(t)$ that triggers the SCR re-

sponse has not been fully exploited by previous methods. Consequently, the interpretability of the decomposition obtained is limited, since true SCR events are difficult to locate in the driver and artificial signals that have no physiological interpretation are introduced by some methods (e.g., [8]) to reduce the error of the model. Furthermore, none of these approaches is able to provide the real-time results required for on-line operation. We addresses all these issues, developing a novel non-negative sparse deconvolution method (SparsEDA), that introduces the following main contributions:

- Multi-scale analysis that addresses the variable time width of the SCR impulses by using an *overcomplete dictionary* that includes responses, $r(t)$, with different widths and selects the appropriate width for each driver's impulse automatically.

- Exploitation of the sparsity of the SCR component (in order to obtain an interpretable decomposition) by formulating the estimation of $d_p(t)$ as a *sparse inference* problem.

- Fast and efficient solution of the resulting optimization problem, thus allowing for on-line extraction of the SNS information.

- Fully automated implementation of the algorithm in Matlab (released through a free web-based repository) that requires only the selection of two easily interpretable parameters by the user.

Following subsection describes the core of the SparsEDA algorithm: the sparse non-negative deconvolution model used. This includes the description of the discrete-time equivalent of Eq. (3.1) in Section 3.2.1; the multi-scale analysis to account for the variable width of the impulses in Section 3.2.2; the approach used to model the SCL in Section 3.2.3; the optimization problem for the joint estimation of the SCL and SCR components in Section 3.2.4; and the post-processing stage in Section 3.2.5. Then, Section 3.3 addresses three issues that are essential to obtain a robust and efficient implementation of the SparsEDA method: the preprocessing

stage (Section 3.3.1); the continuous mode of operation for on-line signal recovery (Section 3.3.2); and the feature extraction (Section 3.3.3). Finally, Section 3.4 validates the method on 100 signals from 100 different subjects and Section 3.5 provides some concluding remarks.

3.2 Proposed Sparse Model

3.2.1 Discrete-Time Model

The discrete-time model that we consider in the sequel is the following:

$$s[n] = s_\ell[n] + d_p[n] * r[n] + w[n]. \tag{3.2}$$

where $n = 0, \ldots, N-1$ with N denoting the total number of samples available; $s_\ell[n]$, $d_p[n]$ and $r[n]$ are obtained through uniform sampling of $s_p(t)$, $d_p(t)$ and $r(t)$ in Eq. (3.1), with a sampling frequency $f_s = 1/T_s$ Hz; and $w[n]$ is an Additive White Gaussian Noise (AWGN) term that takes into account both measurement noise and discretization error.

Note that (3.2) is not the discrete-time equivalent of (3.1) (as obtained by applying the bilinear transformation [26]), but its sampled version. However, it is a standard model [49, 3, 7, 42].

For finite-length sequences, Eq. (3.2) can be expressed more compactly in matrix form as

$$\vec{s} = \vec{s_\ell} + \vec{R}\vec{d_p} + \vec{w}. \tag{3.3}$$

where $\vec{s_\ell} = [s_\ell[0], \ldots, s_\ell[N-1]]^T$, $\vec{R}$ is an $N \times N$ Toeplitz matrix, $\vec{d_p} = [d_p[0], \ldots, d_p[N-1]]^T$ is an $N \times 1$ sparse non-negative vector, and $\vec{w} = [w[0], \ldots, w[N-1]]^T$ is the noise vector. The vector $\vec{d_p}$ is sparse, since its number of non-null elements (indicated by its L_0 pseudo-norm, $\|\vec{d_p}\|_0$) is small compared to its length, i.e., $\|\vec{d_p}\|_0 = L \ll N$ [21]. Note that a universally accepted threshold to define a vector as sparse does not exist, but we may consider that a vector is sparse when it contains less than 10 % of non-null elements (i.e., $L/N < 0.1$). Since $r[n] = 0$ when

$n < 0$ or $n > M - 1$ (see Section 3.2.2),

$$\vec{R} = \begin{bmatrix} r[0] & 0 & \cdots & 0 & 0 & \cdots & 0 & 0 \\ r[1] & r[0] & \cdots & 0 & 0 & \cdots & 0 & 0 \\ \vdots & \vdots & \ddots & & & \ddots & & \\ r[M-2] & r[M-3] & \cdots & r[0] & 0 & \cdots & 0 & 0 \\ r[M-1] & r[M-2] & \cdots & r[1] & r[0] & \cdots & 0 & 0 \\ \vdots & \vdots & & \vdots & \vdots & \ddots & & \\ 0 & 0 & \cdots & 0 & 0 & \cdots & r[0] & 0 \\ 0 & 0 & \cdots & 0 & 0 & \cdots & r[1] & r[0] \end{bmatrix}.$$

Our global aim is inferring both $d_p[n]$ and $s_\ell[n]$ jointly when $r[n]$ (and thus $\vec{R}$) is unknown. In order to achieve this goal, we describe first how to approximate $\vec{R}$ in Section 3.2.2 and then how to model $s_\ell[n]$ in Section 3.2.3.

3.2.2 SCR Model: Multi-scale Analysis

We assume that the sudomotor nerve activity can be described by a biexponential function [3] regarding the specific response triggered by the driver:

$$r(t) = e^{-t/\tau_2} - e^{-t/\tau_1}, \qquad \text{for} \quad t \geq 0. \tag{3.4}$$

According to [3], the optimum performance in their experiments is obtained by setting $\tau_2 = 0.75$ and $\tau_1 = 2$. Therefore, we will use these values in the sequel. Another assumption made in [3] is that the duration of a response varies between one and five seconds. Thus, if τ_1 and τ_2 are fixed, in order to construct several waveforms with different time scales we have to use different sampling periods when discretizing $r(t)$. This leads to an overcomplete dictionary, which is a common approach to circumvent the scale problem in sparse inference methods [21]. Using Q different sampling periods, we have

$$\vec{R}_{SCR} = [\vec{R}_1,\ \vec{R}_2,\ \ldots,\ \vec{R}_Q], \tag{3.5}$$

where $\vec{R}_{SCR}$ is an $N \times NQ$ matrix, and the $\vec{R}_q$ $(q = 1, \ldots, Q)$ are a collection of $N \times N$ matrices (the elements of the dictionary) constructed using a predefined set of waveforms $(r_1[n],\ \ldots,\ r_Q[n])$ with different scales. If these waveforms are

carefully chosen, they will be able to provide a very good approximation of the SCR, even if its scale changes over time. The selection of the element used at each time instant is performed by the $NQ \times 1$ extended vector,

$$\vec{d}_{SCR} = [\vec{d}_1^T,\ \vec{d}_2^T,\ \ldots,\ \vec{d}_Q^T]^T, \tag{3.6}$$

which is still a sparse vector with $\|\vec{d}_p\|_0 \leq \|\vec{d}_{SCR}\|_0 \ll NQ$. Hence, the signal model becomes

$$\vec{s} = \vec{s}_\ell + \vec{R}_{SCR}\ \vec{d}_{SCR} + \vec{w}. \tag{3.7}$$

We propose using $Q = 5$ waveforms,

$$r_i[n] = e^{-nT_s/\tau_{2i}} - e^{-nT_s/\tau_{1i}},$$

for $n = 0, \ldots, M-1$ and $i = 1, \ldots, 5$, with $\tau_{1i} = k_i\tau_1$, $\tau_{2i} = k_i\tau_2$, $k_i \in \{\frac{1}{2},\ \frac{3}{4},\ 1,\ \frac{5}{4},\ \frac{3}{2}\}$, and $M = 10/T_s$ (i.e., M is the number of samples obtained in a time interval of 10 seconds using a sampling period T_s). Therefore, the SCR matrix finally becomes:

$$\vec{R}_{SCR} = [\vec{R}_{T_1},\ \vec{R}_{T_2},\ \vec{R}_{T_3},\ \vec{R}_{T_4},\ \vec{R}_{T_5}], \tag{3.8}$$

where $\vec{R}_{T_i}$ is constructed using $r_i[n]$ for $i = 1, \ldots, 5$. Note that this matrix allows us to cater both for short time-scale processes (e.g., 1-2 seconds) and long time-constant processes (e.g., 3-5 seconds). Furthermore, since we construct the periods $T_1, \ldots, T_5$ as a function of T_s, we are also able to deal with any sampling period automatically. Fig. 3.1 shows the shape of the five different SCR waveforms used to construct $\vec{R}_{SCR}$. Note that all of them correspond to an SNS occurring at the same time instant $t = 0$ (i.e., without any delay), although their effective lengths and the positions of the peaks of the SCR responses are different. The peak of the SCR response is located $\frac{6\ln(8/3)}{5}k_i$ seconds after the SCR event that triggered the response. For the $k_i \in \{\frac{1}{2},\ \frac{3}{4},\ 1,\ \frac{5}{4},\ \frac{3}{2}\}$ used in Fig. 3.1 this corresponds approximately to $\{0.5885,\ 0.8827,\ 1.1770,\ 1.4712,\ 1.7655\}$ seconds, respectively.

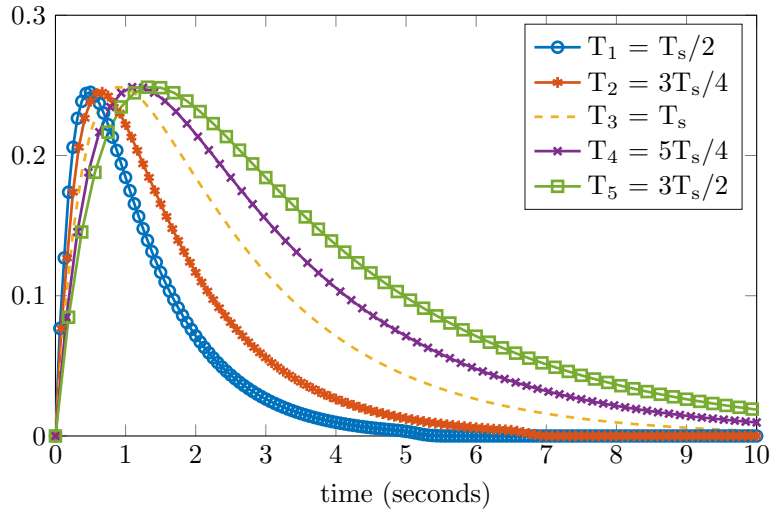

Figure 3.1: Multi-Scale SCR waveforms ($r_1[n]$, ..., $r_5[n]$), obtained discretizing $r(t)$ in Eq. (3.4) using five different periods: $T_1 = T_s/2$, $T_2 = 3T_s/4$, $T_3 = T_s$, $T_4 = 5T_s/4$, and $T_5 = 3T_s/2$. All of them correspond to an SNS occurring at the same time instant $t = 0$.

3.2.3 SCL Model: Taylor Series Expansion

In order to approximate the SCL in a simple and efficient way, we propose to use a first order Taylor series expansion:

$$\vec{s}_\ell = [\vec{1}/||\vec{1}||_2 \;\; \boldsymbol{\ell}/||\boldsymbol{\ell}||_2 \;\; -\boldsymbol{\ell}/||\boldsymbol{\ell}||_2]\, \vec{d}_{SCL} = \vec{R}_{SCL}\vec{d}_{SCL}, \tag{3.9}$$

where $\mathbf{1} = [1, \ldots, 1]^T$ and $\boldsymbol{\ell} = [0, 1, \ldots, N-1]^T$ are constant and linearly increasing $N \times 1$ column vectors, respectively; $\|\cdot\|_2$ denotes the L_2 norm, so $||\vec{1}||_2 = \sqrt{N}$ for instance; $\vec{R}_{SCL}$ is the $N \times 3$ matrix built using those column vectors; and $\vec{d}_{SCL}$ is a non-negative coefficients vector.

3.2.4 Joint SCL and SCR estimation

The standard approaches to GSR signal analysis in the literature are based on the sequential extraction of $s_\ell(t)$ and $s_p(t)$. On the one hand, $s_\ell(t)$ can be estimated as an average of $s(t)$ over short intervals (10 to 100 seconds [3, 8]), and then subtracted from $s(t)$ in order to obtain $s_p(t)$. Alternatively, $s_p(t)$ can be obtained from $s(t)$ through a high pass filter [25], and then, if desired, $s_\ell(t)$ can be obtained

again by subtraction. Either way, as pointed out in [7], this sequential extraction tends to underestimate the SCR component.

Here, it is proposed to estimate both the SCL and the SCR components simultaneously, exploiting the fact that $\vec{R}_{SCL}$ and $\vec{R}_{SCR}$ can be combined into a single $N \times (NQ + 3)$ matrix: $\vec{R}_T = [\vec{R}_{SCL}\ \vec{R}_{SCR}]$. Hence, can be rewritten Eq. (3.7) more compactly as

$$\mathbf{s} = \vec{R}_T \vec{d}_T + \vec{w}, \tag{3.10}$$

where $\vec{d}_T = [\vec{d}_{SCL}^T\ \vec{d}_{SCR}^T]^T \in \mathbb{R}^{NQ+3}$. This is the joint SCL-SCR model that we use in the sequel to perform the joint estimation of the SCL and SCR components.

The proposed solution is based on the following key characteristics of the skin conductance response [99, 52]:

- The driver, $d_p(t)$, represents sudomotor nerves activations, and thus it corresponds either to non-negative deflections (during states of activity) or remains equal to zero otherwise.
- A single impulse corresponds to each SNS act [7] and triggers an SCR response that typically lasts from 1 to 5 seconds [7].
- The sudomotor impulses arrive as discrete and separate (i.e., non-overlapping) events, implying that $\vec{d}_{SCR}$ should be sparse in time.

These facts lead us to consider a *non-negative sparse driver*, with the constraint that $d_T(i) \geq 0$ for $1 \leq i \leq N$, which is characterized by a zero baseline and occasional (i.e., sparse) discrete positive impulses with a compact support. Hence, the estimation of $\vec{d}_T$ can be formulated as the following constrained optimization problem:

$$\hat{\vec{d}}_T = \underset{\vec{d}_T}{\arg\min} \quad \|\vec{s} - \vec{R}_T \vec{d}_T\|_2^2 \tag{3.11a}$$

$$\text{subject to} \quad d_T(i) \geq 0\ \forall i \tag{3.11b}$$

$$\|\vec{d}_T\|_0 \ll NQ \tag{3.11c}$$

Eq. (3.11a) corresponds to the minimization of the mean squared error Mean Square Error (MSE) between the available signal and the reconstructed one, Eq.

(3.11b) is the non-negativity constraint, and Eq. (3.11c) is the sparsity constraint. Since the L_0 pseudo-norm is untractable from a mathematical point of view, the sparsity constraint in Eq. (3.11c) can be imposed using an L_1 regularization term, that leads to the following non-negative version of the Least Absolute Shrinkage and Selection Operator (LASSO) [96]:

$$\hat{\vec{d}}_T = \underset{\vec{d}}{\arg\min} \quad \|\vec{s} - \vec{R}_T \vec{d}_T\|_2^2 + \lambda \|\vec{d}_T\|_1 \tag{3.12a}$$

$$\text{subject to} \quad d_T(i) \geq 0 \; \forall i \tag{3.12b}$$

which can be solved efficiently using the Least Angle Regression (LARS) algorithm [20].

Note that the regularization parameter, λ, controls the amount of sparsity in the reconstruction: the larger the value of λ the sparser the signal obtained. However, λ has no clear interpretation in terms of GSR signals, and thus it can be difficult for the user to find an appropriate value for it. Instead, since LARS is a greedy algorithm, we propose to replace the choice of λ by the selection of a stopping rule that can be set much more easily by users without a detailed technical knowledge of the algorithm. For instance, we stop the optimization when the residual of the GSR reconstruction is less than a pre-defined value (i.e., $\|\vec{s} - \vec{R}_T \hat{\vec{d}}_T\|_2^2 \leq \epsilon$) or a maximum number of iterations $K_{\max}$ have been performed. Furthermore, since a final post-processing stage is performed (see Section 3.2.5) to remove redundant impulses, the user can simply set values of ϵ and $K_{\max}$ which ensure that all the potential impulses have been discovered by LARS (e.g., in the simulations we have used $\epsilon = 10^{-4}$ and $K_{\max} = 40$), and then control the degree of sparsity during the post-processing.

3.2.5 Post-Processing

The goal of the post-processing stage is to obtain a driver signal, $d_p(t)$, which is as sparse as possible. In order to achieve this goal, we propose to apply a greedy algorithm that eliminates weak impulses which are too close to stronger impulses, following a similar approach to [72, 50]. These impulses are included by LARS

in order to decrease the MSE, but are useless from a physiological point of view and hinder the interpretability of the recovered signals. In summary, the proposed approach is the following:

1. Initialize the set of accepted impulses as the empty set: $\mathcal{A} = \emptyset$.

2. Sort the elements of $\vec{d}_{SCR}$ in descending order according to their L_1 norm. Hence, the resulting ordered vector, $\vec{d}_{ord}$, fulfills that

$$\|\vec{d}_{ord}(1)\|_1 \geq \|\vec{d}_{ord}(2)\|_1 \geq \cdots \geq \|\vec{d}_{ord}(N)\|_1.$$

   Note that, since $\vec{d}_{SCR}$ is sparse, only the first $L_{SCR} \ll NQ$ elements of $\vec{d}_{ord}$ are different from zero.

3. For $i = 1, \ldots, L_{SCR}$:

   (a) If the location of $\vec{d}_{ord}(i)$ is not within $T_{\min}$ seconds (i.e., $N_{\min} = T_{\min} f_s$ samples) of an existing impulse in $\mathcal{A}$, add it to the set of accepted impulses.

   (b) Otherwise, discard it.

4. Discard the accepted impulses whose L_0 norm lies below the following threshold:

$$\gamma = \rho \max \|\vec{d}_{SCR}\|_1,$$

   where $0 < \rho < 1$ is a user specified parameter that can be used to control the final sparsity of the solution obtained.

The minimum distance constraint enforced by the previous algorithm could also be included within the optimization problem, as shown by the Cross-Products LASSO algorithm [51]. However, this leads to a substantial increase in computational cost (since the resulting problem is not convex anymore), that would prevent the on-line implementation that we are seeking here.

3.3 Practical Implementation

3.3.1 Preprocessing

The problem of using wearable sensors make the quality of the signal should decrease due noise and/or artifacts and out-layers. These external factors can be generated because there is no contact between the electrode and the skin or excessive movements. In case that exists lots of external factors, a new method developed by Taylor et. al [94] regenerate the GSR signal. In order to remove these artifacts, Sara Taylor et al. [94] developed a machine learning algorithm to detect automatically Electrodermal Activity (EDA) artifacts that will be used before applying our novel SparsEDA algorithm. This method takes segments of 5 seconds and classifies them either as artifacts or as valid GSR signals. In those slots that are classified as artifacts, the signal is replaced by a polynomial regression of order 1 between the last non-artifact point in previous slots and the first non-artifact sample in subsequent slots, and no further processing is performed.

Besides the artifact removal stage, the complete signal is resampled to 8 Hz if the sampling frequency, f_s, is higher than 8 Hz. This resampling does not have any influence on the signal's quality, since SCR waveforms can be perfectly represented using $f_s = 8$ Hz (or even $f_s = 4$ Hz), but allows us to reduce notably the computation time.

3.3.2 Continuous-mode Operation

The final goal of the SparsEDA method is being able to extract EDA-related features continuously using shorter signal sets of $N = W + M + 1 < L$ samples, where M is the length of the waveforms used to construct the SCR dictionary and L is the total number of samples available of the GSR signal. This continuous-mode operation allows us to deal with large signals of arbitrary length (since the approach is applied on segments of fixed length) and even to process signals on-line (i.e., as they are being acquired) in real-time or quasi-real-time. The SparsEDA algorithm incurs in a fixed processing delay equal to the time shift used (W or $W/3$), but

$$\vec{R}'_{SCL} = \begin{bmatrix} \bar{\ell}_1(1) & -\bar{\ell}_1(1) & 0 & 0 & 0 & 0 \\ \vdots & \vdots & \vdots & \vdots & \vdots & \vdots \\ \bar{\ell}_1(\frac{W}{3}) & -\bar{\ell}_1(\frac{W}{3}) & 0 & 0 & 0 & 0 \\ \bar{\ell}_1(\frac{W}{3}+1) & -\bar{\ell}_1(\frac{W}{3}+1) & \bar{\ell}_2(1) & -\bar{\ell}_2(1) & 0 & 0 \\ \vdots & \vdots & \vdots & \vdots & \vdots & \vdots \\ \bar{\ell}_1(\frac{2W}{3}) & -\bar{\ell}_1(\frac{2W}{3}) & \bar{\ell}_2(\frac{W}{3}) & -\bar{\ell}_2(\frac{W}{3}) & 0 & 0 \\ \bar{\ell}_1(\frac{2W}{3}+1) & -\bar{\ell}_1(\frac{2W}{3}+1) & \bar{\ell}_2(\frac{W}{3}+1) & -\bar{\ell}_2(\frac{W}{3}+1) & \bar{\ell}_3(1) & -\bar{\ell}_3(1) \\ \vdots & \vdots & \vdots & \vdots & \vdots & \vdots \\ \bar{\ell}_1(W) & -\bar{\ell}_1(W) & \bar{\ell}_2(\frac{2W}{3}) & -\bar{\ell}_2(\frac{2W}{3}) & \bar{\ell}_3(\frac{W}{3}) & -\bar{\ell}_3(\frac{W}{3}) \\ 0 & 0 & 0 & 0 & 0 & 0 \\ \vdots & \vdots & \vdots & \vdots & \vdots & \vdots \\ 0 & 0 & 0 & 0 & 0 & 0 \end{bmatrix} \tag{3.13}$$

afterwards it is able to return the SCL and SCR values almost instantaneously. In order to describe this mode of operation, let us set $M = 10/T_s$ (i.e., the duration of the SCR waveforms is 10 seconds), $W = 60/T_s$, and refer to the current slot being processed (whose duration is 70 seconds) as the *active set*.

First of all, a *naive implementation* of the SparsEDA algorithm for large/on-line signals is straightforward:

1. Extend the signal by adding M samples before the first one and W samples after the last one. These samples are required to ensure that the whole signal is properly processed and can take arbitrary values. For instance, we simply replicate the first and last samples in the signal M and W times, respectively, to perform this extension.

2. Set the first N samples of the extended signal as the active set.

3. Apply the SparsEDA method described in Section 3.2 on the current active set, obtaining an estimate of its SCL and SCR components for the first W samples.

4. Keep shifting the active set by W samples and repeating the previous stage

until all the samples in the original GSR signal have been processed.

5. Discard the SCL and SCR components corresponding to the samples added at the beginning and the end of the signal.

However, this naive approach does not ensure the continuity of the signal among the different segments for the SCL component and can lead to high MSE values. In order to promote the continuity, we propose to divide the active set into three continuous sets, composed of $\frac{1}{3}W$ samples each one, and to use a modified $\vec{R}_{SCL}$ matrix, $\vec{R}'_{SCL}$. This matrix, shown in Eq. (3.13), is composed of W rows (i.e., the length of the active set) and six columns that correspond, respectively, to the positive and negative versions of the SCL model for each of the three segments of the active set. In Eq. (3.13), the $\boldsymbol{\ell}_i$ are linearly increasing column vectors ($\boldsymbol{\ell}_1$ from 0 to 1 with a length $L_1 = W$, $\boldsymbol{\ell}_2$ from 0 to 2/3 with a length $L_2 = 2W/3$, and $\boldsymbol{\ell}_3$ from 0 to 2/3 with a length $L_3 = W/3$); $\bar{\boldsymbol{\ell}}_i = \boldsymbol{\ell}_i / \|\boldsymbol{\ell}_1\|_2$ are the normalized vectors (w.r.t. the L_2 norm of $\boldsymbol{\ell}_1$); and $\bar{\ell}_i(k)$ denotes the k-th element ($k = 1, 2, \ldots, L_i$) of $\bar{\boldsymbol{\ell}}_i$. This construction of the matrix enforces the continuity among those three segments, since a discontinuity results in an increase in the MSE. Hence, the *continuous-mode operation* SparsEDA algorithm proposed is finally:

1. Extend the signal by adding M samples before the first one and W samples after the last one.

2. Set the first N samples of the extended signal as the active set.

3. Subtract the value of the first sample, and apply the SparsEDA method described in Section 3.2 on the current active set, using a matrix $\vec{R}'_T = [\vec{R}'_{SCL}\ \vec{R}_{SCR}]$, with $\vec{R}'_{SCL}$ given by (3.13) and $\vec{R}_{SCR}$ given by (3.8), thus obtaining an estimate of the SCL and SCR components for the first $W/3$ samples. Note that (3.13) does not contain the offset term for the Taylor series expansion used to model the SCL. Hence, we subtract the first sample of the active set to ensure that the line used to model the SCL starts at 0. Add back the value of the subtracted sample to obtain the final solution.

4. Keep shifting the active set by $W/3$ samples and repeating the previous stage until all the samples in the original GSR signal have been processed.

5. Discard the SCL and SCR components corresponding to the samples added at the beginning and the end of the signal.

Note that the difference w.r.t. the naive implementation lies in steps 3 and 4 (using a modified matrix R'_T and shifting the active set by $W/3$ samples instead of W).

The proposed SparsEDA algorithm has been made freely available (altogether with the results presented in Section 3.4, which are provided in a `.mat` file) through a well-known web-based code repository (`https://github.com/fhernandogallego/sparsEDA`) and can also be found in the author's web-page (`http://www.tsc.uc3m.es/~fhernando/Research.html`). The code, which has been developed in MATLAB, is based on the implementation of the LASSO algorithm provided by [101].

3.3.3 Feature Extraction

The SparsEDA algorithm allows us to extract two GSR components (features) that should be interesting for SNS studies:

- **Tonic component (SCL):** The slope is related to the level of attention of the subject. If the patient is concentrated and/or involved in a task, an increasing slope should be observed [32]. Otherwise, the SCL slope should either decrease or remain constant.

- **Phasic component (SCR):** This is the indicator of SNS reactions. The proposed method allows us to extract both their locations and durations. Furthermore, the sparsity of the resulting driver enhances its interpretability, whereas the post-processing stage allows us to avoid false alarms.

An example of the application of the SparsEDA method is shown in Fig. 3.2. The input is a GSR signal of length $N = W + L + 1$ (in blue), and the results (features) are a sparse driver signal of length W (displayed as black impulses), the

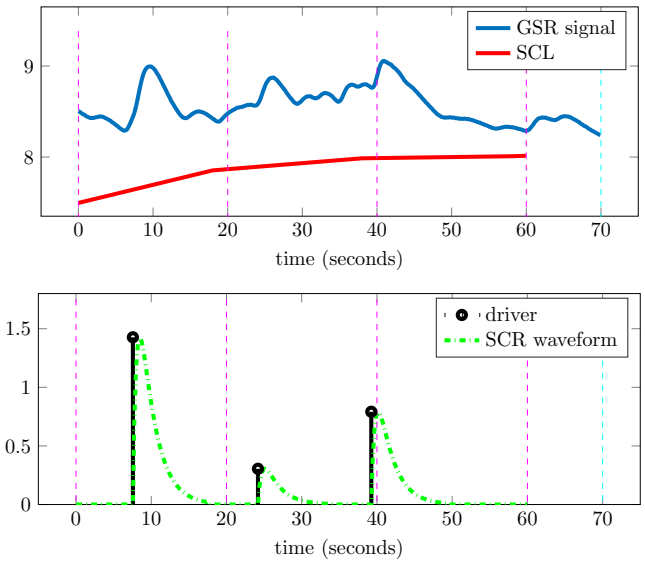

Figure 3.2: Signal extraction example using SparsEDA. **(Top)** A GSR signal (blue) of duration equal to 70 seconds (i.e., length $L = 70/T_s$ samples), and the SCL signal (red) obtained by SparsEDA. **(Bottom)** Sparse driver obtained (black) and the SCR waveform for each mark (dash-dotted green).

corresponding SCR component of length W (in green), and the low-frequency SCL components for each length $\frac{1}{3}W$ set (in red) with their associated slope. Purple vertical lines separate each $\frac{1}{3}W$ set, whereas the cyan line indicates the end of the signal.

3.4 Results

First of all, we show the qualitative behavior of SparsEDA on a record acquired at $f_s = 16$ Hz with length equal to 400 seconds that is freely available at [48]. Fig. 3.3 compares the SCL and SCR components extracted by the novel SparsEDA algorithm (without decreasing the sampling rate) and two alternative approaches: the Continuous Decomposition Analysis (CDA) technique introduced in [7] (CDA Ledalab), and the convex approach proposed in [27] (cvxEDA). Regarding the SCL component, it can be seen that SparsEDA retrieves an SCL component which is very similar to the one returned by cvxEDA, and both of them lie below the SCL

component obtained using CDA Ledalab. However, the main difference can be appreciated in the SCR component. On the one hand, the SCR signal returned by CDA Ledalab is not at all sparse and the driver's impulses are very difficult to locate. On the other hand, although cvxEDA returns a sparser SCR component, it still contains too many activations to be useful for the task of locating the driver's impulses and counting their number. Finally, SparsEDA returns a truly sparse SCR signal (with a degree of sparsity that can be easily controlled by the user, as described in Section 3.2) that contains the main impulses of the driver and which is much more interpretable than the other two from a physiological point of view.

Then, in order to show the versatility of the proposed approach, we have compared the performance of the novel SparsEDA method with the same two algorithms as before: CDA Ledalab [7] and cvxEDA [27]. The simulations have been performed on a database composed of 100 GSR signals from 100 different patients acquired at several sampling rates from 4 Hz to 128 Hz, with different sensors and a wide range of signal lengths. 50 signals were recorded within the ES3 project [2], using Medicom MTD sensors [70] and following the procedure described in [34]. The rest were recorded in our laboratory using: the Empatica E4 sensor [23] (5 signals), Microsoft's Band 2 [71] (5 signals), Qsensor [1] (35 signals), and Shimmer3 [91] (5 signals). Regarding our SparsEDA algorithm, we have used the same parameters as before: $\epsilon = 10^{-4}$, $K_{\max} = 40$ iterations, $N_{\min} = \frac{5}{4} f_s$ samples, and $\rho = 0.025$. All the signals have been preprocessed using the web-based method proposed in [94], segmenting them into slots of 5 seconds that correspond either to a valid GSR signal or artifact/noise, and replacing the slots that were labelled as artifacts by a linear regression. After this preprocessing stage, each signal was processed using the three aforementioned algorithms, extracting the SCR and SCL components.

Table 5.1 summarizes the characteristics of the six groups of data used in the simulations (number of signals, sampling rate, type of sensor used and duration [mean and standard deviation (std.)]), altogether with the results obtained: the relative MSE for SparsEDA (mean and std.) and the computation time for the three algorithms tested (mean and std.). Note that sampling rates larger than 8

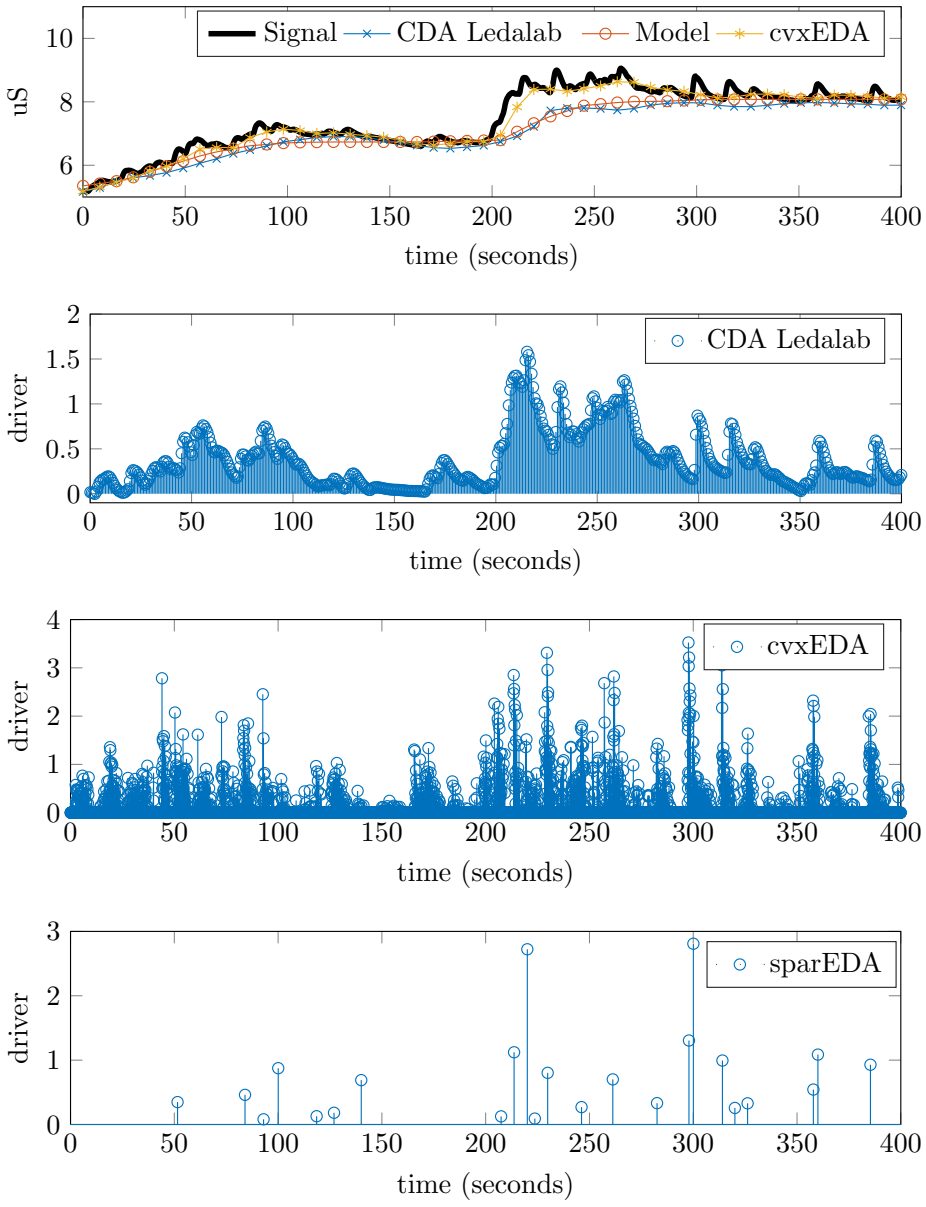

Figure 3.3: Signal processing for GSR signal feature extraction using a sampling rate $f_s = 16$ Hz. (a) Black line representing the GSR signal and several lines with markers showing different SCL approximations: CDA Ledalab (blue crosses), SparsEDA (red circles) and cvxEDA (yellow stars). (b) CDA Ledalab driver obtained using 4 iterations of the optimization tools. (c) Driver obtained using cvxEDA. (d) Driver obtained using SparsEDA with $\epsilon = 10^{-4}$, $K_{\max} = 40$ iterations, $N_{\min} = \frac{5}{4} f_s = 20$ samples, and $\rho = 0.025$.

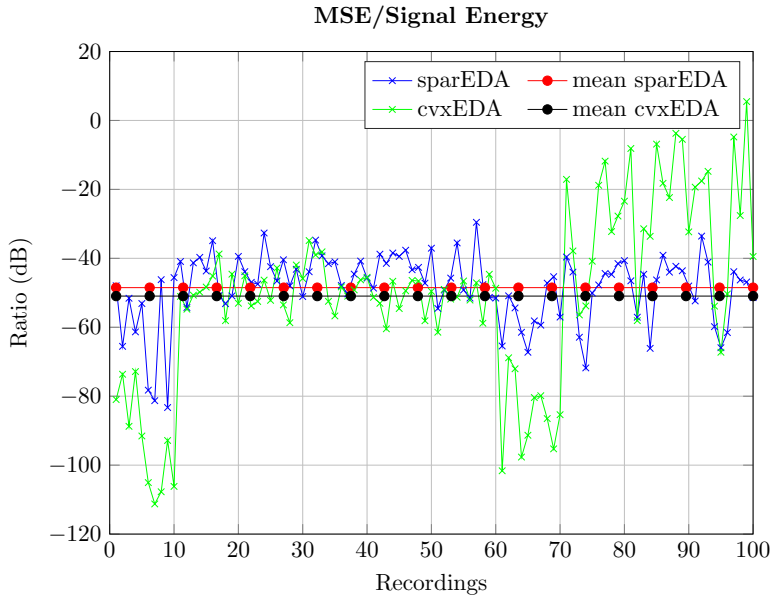

Figure 3.4: Ratio (dB) between the MSE and the signal energy for the 100 signals in the database and two of the methods compared: SparsEDA and cvxEDA. Blue and green lines show the ratio of SparsEDA and cvxEDA for each particular signal in the database, whereas the horizontal red and black lines display their average values.

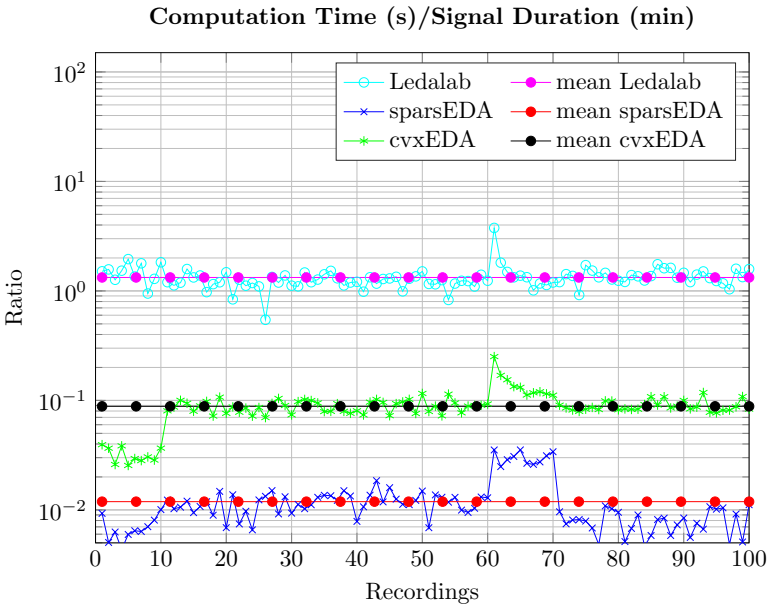

Figure 3.5: Ratio between the computation time (in seconds) and the signal's duration (in minutes) for the 100 signals in the database and the three methods compared: SparsEDA, CDA Ledalab and cvxEDA. Cyan, blue and green lines show the ratio of SparsEDA, CDA Ledalab and cvxEDA for each signal in the database, whereas the horizontal purple, red and black lines display their average values.

Hz has been re-sampled to 8 Hz for all of the methods. A detailed analysis of the results obtained is provided in the sequel:

- Fig. 3.4 displays the MSE obtained by SparsEDA and cvxEDA for each record. Let us remark that the main goal of SparsEDA is obtaining an interpretable SCL/SCR decomposition in a small amount of time (i.e., attaining a good balance between computation time and MSE), not fitting the SCL and SCR components in order to obtain a zero remainder. However, very good values of MSE are attained: from a minimum value of -83.29 dB to a maximum value of -29.55 dB, with an average MSE equal to -48.50 dB. Although cvxEDA attains lower MSE values (from -111.26 dB to 5.47 dB, with -50.95 dB on average), this is hindered by the much lower interpretability of the resulting SCR signal (as shown in Fig. 3.3 and discussed below).

- The MSE obtained by CDA Ledalab is not included in Fig. 3.4 because it is fitted to zero by using a non-sparse SCR component (which is not physiologically interpretable) that contains all the elements of the signal that do not belong to the SCL.

- The computation time is summarized for each method in Table 3.1, showing that SparsEDA is always faster than cvxEDA, and both of them are much faster than CDA Ledalab. Fig. 3.5 delves deeper into this important feature, showing the ratio between the computation time (in seconds) and the duration of the signal (in minutes). The average values of the ratios, which are also displayed, are 1.327 for CDA Ledalab, 0.088 for cvxEDA and 0.012 for SparsEDA (i.e., on average SparsEDA is 7.42 times faster than cvxEDA and 111.58 times faster than CDA Ledalab).

- The level of sparsity in the SCR component is directly related to the interpretability of the decomposition obtained: the sparser the signal the more interpretable from a physiological point of view. In this sense, while SparsEDA attains an average sparsity of 0.287% (percentage of non-zero values out of the total number of samples), the other two methods are non-sparse, always

returning 100% non-zero values (cvxEDA contains many samples with small but non-null values).

- Confidence intervals and p-values comparing SparsEDA with CDA Ledalab and cvxEDA (both in terms of relative MSE and computation time) have been computed and are displayed in Table 3.2. These values have been computed through the t-test (using Matlab's `ttest2` function) on the hypothesis that the mean of the two distributions of the results (i.e., those of SparsEDA and the compared algorithm) are equal. From the p-values obtained (well below the 0.05 threshold typically used) we can see that both the differences in relative computation time and MSE are statistically significant. However, note that the loss in MSE attained by SparsEDA is small with respect to the decrease in computation time, as shown in Figs. 3.4 and 3.5 and evidenced by the p-values in Table 3.2.

#	Sampling Rate	Sensor	Duration (minutes)		MSE/SE (dB)		Computation Time (seconds)					
							CDA Ledalab		SparsEDA		cvxEDA	
			Mean	Std	Mean	Std	Mean	Std	Mean	Std	Mean	Std
1-5	4 Hz	Empatica E4	50.00	00.00	-55.90	7.27	78.29	12.36	0.31	0.09	1.65	0.34
6-10	5 Hz	Microsoft Band 2	33.99	19.50	-66.92	19.28	52.51	41.65	0.28	0.23	1.09	0.78
11-60	8 Hz	Medicom MTD	39.43	05.47	-44.03	5.97	48.53	10.37	0.46	0.11	3.50	0.72
61-65	16 Hz	Qsensor	32.62	22.00	-59.88	7.07	41.15	53.46	0.29	0.24	2.73	2.71
66-70	128 Hz	Shimmer 3	9.90	00.00	-53.42	6.62	11.56	1.14	0.14	0.03	1.13	0.03
71-100	8 Hz	Qsensor	9.89	00.00	-48.92	9.20	72.80	10.13	0.41	0.10	4.70	0.55

Table 3.1: Summary of the characteristics of the 100 GSR records used in the simulations and the results obtained. They are separated into six groups according to the sampling rate and the sensor. The duration (mean and standard deviation [std.]) of each group are also shown. Relative MSE (MSE/Signal Energy (SE)) is only shown for SparsEDA. Computation time (mean and std.) is shown for the three algorithms compared: SparsEDA, CDA Ledalab and cvxEDA.

#	Sampling Rate	MSE/SE SparsEDA vs cvxEDA			CT/SD SparsEDA vs CDA Ledalab			CT/SD SparsEDA vs cvxEDA		
		p-values	conf. int.		p-values	conf int.		p-values	conf. int.	
			lower	upper		lower	upper		lower	upper
1-5	4 Hz	9.09 e-04	14.09	37.20	6.21 e-07	-1.81	-1.32	2.96 e-05	-0.03	-0.020
6-10	5 Hz	3.40 e-03	16.54	58.84	2.39 e-09	-1.81	-1.05	8.26 e-07	-0.027	-0.019
11-60	8 Hz	8.67 e-06	3.16	7.79	6.77 e-68	-1.25	-1.15	4.01 e-68	-0.080	-0.073
61-65	16 Hz	7.30 e-03	9.35	43.49	3.10 e-10	-2.98	-0.86	2.50 e-04	-0.18	-0.090
66-70	128 Hz	4.81 e-05	22.68	41.41	1.90 e-08	-1.25	-1.02	2.07 e-10	-0.091	-0.081
71-100	8 Hz	6.58 e-07	-28.89	-13.63	-2.21 e-43	-1.43	-1.30	-3.90 e-45	-0.085	-0.077

Table 3.2: Statistical comparative between SparsEDAand cvxEDAin terms of relative MSE/SE and SparsEDAversus cvxEDAand CDA Ledalab in terms of CT/SD. P-values and confidence intervals (lower and upper limits) are displayed to show the significant differences. MSE/SE = MSE/Signal Energy. CT/SD = Computation Time (s)/Signal Duration (min).

3.5 Conclusions

We have developed a novel feature extraction method for GSR signals: the SparsEDA algorithm. The main contributions of SparsEDA are the joint estimation of the SCL and SCR components, the multi-scale analysis using an over-complete dictionary, the retrieval of a sparse driver for the SCR component, and the efficient implementation of a fully automated, continuous-mode operation algorithm for on-line processing. The proposed approach has been tested on a database of 100 GSR records from 100 different patients acquired using different sensors and sampling rates, confirming its good performance in terms of relative MSE (-48.50 dB) and computation time (1–2 orders of magnitude lower than other existing algorithms like CDA Ledalab and cvxEDA). Furthermore, the interpretability of the SCR component extracted is enhanced w.r.t. previous approaches, thanks to the sparsity of the driver (unlike both CDA Ledalab and cvxEDA, which return non-sparse drivers) and the lack of artificial non-interpretable signals introduced to minimize the MSE (as done by CDA Ledalab). In summary, SparsEDA confirms the feasibility of developing a fast and fully automated method for extracting the GSR components from large EDA records. One possible future line would be embedding this software within a wearable sensor or a real-time mobile application to detect SNS symptoms using driver activations. Another potential application would be integrating it within medical software to detect stress reactions while an patient is performing some activity.

In the literature, several Bayesian approaches can be also found, tackling these problems. They are based on the implementation of rejection sampling methods [56, 18, 57, 62], importance sampling techniques [59, 13, 22, 60], Markov Chain Monte Carlo (MCMC) algorithms [67, 66, 61] and combination of them [58, 65, 63, 64].

4

Stress Features

Short-term stress influences in a variety of physiological signals as is mentioned in Section 2.4. Depending on the activity and the person, stress may sometimes manifest itself in one, more than one or no physiological signal. This chapter presents several stress features obtained analyzing biological signals. The criteria selection for each feature is based on two assumptions: features used in the past for another researchers and the acquisition should be non-intrusive.

The methodology to extract stress feature used in the literature is to select some phisiological signals, analyze them and apply machine learning algorithms to make a robust model. Some examples of past feature stress extraction models are: D. Wu et al. [104] captured physiological responses from: Galvanic Skin Response (GSR), respiration, electroencephalogram and electrocardiogram for identification and classification into several stress levels. Another case was Zhai and Barreto

[107], who acquired different affective features: GSR, Blood Volume Presure (BVP) and pupil diameter to differentiate states (relax or mental stress) in computers user. Speech also plays a role in detecting stress as can be depicted form [17] where stress is estimated using pitch and speech energy features and [74] where Log Frequency Power Coefficients (LFPC) are used to detect stress and emotion.

The methodology to analyze each signal is to calculate in time windows of the same length, 60 seconds, each feature due Autonomous Nervous System (ANS) activations are provoked slowly. Summarize each feature in a value of one minute is enough sample to extract stress information [82]. If any feature provides more samples per 60 seconds, the average is calculated to obtain only one number per minute.

4.1 Heart Rhythm

The most common signal obtained from heart rhythm activity is the heart rate. It shows the duration of one cardiac cycle (Inter-Beat (RR) interval) calculated in average for one minute length $HR = 60/RR$ and measured in beats/minute. Mostly wearable sensors provide this rate, usually used in fitness activities or only with the end of inform the user. But in medical health applications, fluctuations in beat-to-beat periods are commonly referred to Heart Rate Variability (HRV) [16] which analyses the physiological phenomenon of the oscillation in the interval between consecutive heart beats [15].

All of the heart rhythm features used for other authors [5, 92, 44, 30] are calculated as a statistical computation of the beat-to-beat. The proposed features can be divided in time or frequency domain and are also described in [15]. On one hand, the following features are computed in the time domain:

- Standard Deviation of NN Intervals (SDNN). It is computed following the expression:

$$\text{SDNN}_i = \sqrt{\frac{1}{n-1}\sum_{j=1}^{n}(RR_j - \overline{RR})^2}$$

where RR_J is the inter-beat (RR) interval, $\overline{RR}$ is the mean of the RR over the window of 60 seconds, and n is the number of RR points in the window. The sample rate for heart rate is 1 Hz, so the number of samples is 60 samples per window.

- Root Mean Square of Successive Differences (RMSSD). It can be obtained as the square root of the mean of the sum of the squares of differences between adjacent intervals. It can be expressed as:

$$\text{RMSSD}_i = \sqrt{\frac{1}{n-1}\sum_{j=1}^{n}(RR_{j+1} - RR_j)^2}$$

- Pairs of adjacent RR intervals differing by more than 50 ms (pNN50). It is computed as the the number of pairs satisfying the condition in the analysis period divided by the by the total number of all RR intervals. It is denoted as:

$$\text{pNN50}_i = P(|RR_{j+1} - RR_j| > 50ms)$$

On the other hand, the following feature is computed in the time domain:

- LF/HF ratio (Low Frequency/High Frequency). It is computed as the ratio between the power in the low frequency LF_{HRV} and high frequency HF_{HRV} frequency bands. It is computed following the expression:

$$\text{LF/HF ratio}_i = \frac{\int_{0.04Hz}^{0.15Hz} f(\lambda)d\lambda}{\int_{0.15Hz}^{0.40Hz} f(\lambda)d\lambda}$$

where $f(\lambda)$ spectrum of the RR. This feature reflect the degree of sympathovagal balance with a higher ratio.

4.2 Electrodermal Activity

This feature extraction model employs our previously presented GSR feature extraction method explained in chapter 3. This model divide the GSR signal into two components:

- **Skin Conductance Lelvel (SCL)**: This is related to the level of attention of the subject. If a person is concentrated and/or involved in a task, an increasing slope should be observed [32]. Otherwise, the SCL slope should either decrease or remain constant.

- **Skin Conductance Response (SCR)**: This is the indicator of sympathetic reactions (smaller than 10 seconds). This method allows to extract their locations and durations. Furthermore, the sparsity of the resulting signal enhances its interpretability, whereas the post-processing stage allows to avoid false alarms.

The two components are computed for each $i-th$ interval obtaining the interval tonic component SCL_i and interval phasic component SCL_i. Given those components the following features can be computed:

- SCL slope. It represents the slope of a linear regression of the 60 seconds fo the time window.

$$m_i = \frac{SCL_{i+1} - SCL_i}{t_{i+1} - t_i}$$

  where SCL are the values of the slope for the i^{th} interval and t is the elapsed time (in this case are always 1 minute).

- SCR: It counts the number peaks that appear in the 60 seconds interval.

$$SCR_i = \sum (d_i > 0)$$

  where d is the driver obtained for each i^{th} interval (non-zero values are sympathetic reactions).

- Driver Area (DA): is the sum of each driver values in the 60 seconds interval.

$$DA_i = \sum d_i$$

  and finally values of the driver for each i^{th} interval are summed.

4.3 Speech Features

There are different ways to capture information contained in speech relevant to stress detection. This work use a simplified feature set based on the InterSpeech 2009 Emotion [83] and Paralinguistic Challenge [84] features. The features are extracted with the openSMILE toolbox [24].

Five low-level descriptors of voice quality and pitch are computed: the estimated pitch, the voicing probability, the Jitter and the Shimmer. Finally the smoothed energy computed using the overlapping time frames is also included.

- The pitch is defined as the relative highness or lowness of a tone as perceived by the ear, which depends on the number of vibrations per second produced by the vocal cords. It represents the vibration frequency of the vocal cords during the sound productions (like vowels, for example). It is computed following [19, 95], using the autocorrelation function, the correlation of a variable with itself over time as:

$$R(k) = \sum m = 0k - 1x(m)x(m+k) \tag{4.1}$$

  We then compare the result for $Fs/350 <= K <= Fs/80$, and the pitch will be computed as $f0 = K + \frac{fs}{350}$

- The voicing probability indicate the percentage of unvoiced and voiced energy in a speech signal. It is also obtained using the same estimated fundamental frequency. The voicing frames are computed taking a threshold: $R > 0.3Rn0$ where $R = \max_n Rn0$.

- The Shimmer is computed as the local (frame-to-frame) amplitude deviations between pitch periods. It is the average absolute difference between the amplitudes of consecutive periods, divided by the average amplitude. It can be expressed as:

$$shim = \frac{\frac{1}{N-1}\sum_{i=1}^{N-1}|A_i - A_{i+1}|}{\frac{1}{N}\sum_{i=1}^{N} A_i}, \tag{4.2}$$

  where A_i is the extracted amplitude and N is the number of extracted fundamental frequency periods.

- The Jitter is also computed as the local (frame-to-frame) pitch period length deviations. It is the average absolute difference between consecutive periods, in seconds. It can be expressed as:

$$jitt = \frac{1}{N-1} \sum_{i=1}^{N-1} |T_i - T_{i-1}|, \tag{4.3}$$

  where Ti is the extracted period lengths of the signal and N is the number of extracted periods.

- The smoothed energy computed using the overlapping time frames.

In order to combine the speech features with the previously presented hearth rhythm and electrodermal activity features the arithmetic mean of the features contour is performed in a 60 second basics.

4.4 Hormone Analysis

Stress situations increases cortisol levels by the adverse effects of blood sampling. Instead of the other features, the methodology to measure cortisol levels requires more time and also varies in a time line of minutes, even hours. Past authors [103, 98, 81, 93, 55] have elicited stress while the subject is performing an activity and then, they have compared the levels of cortisol before and after the experiment.

The methodology to calculate this feature is to cooler a cortisol value right before and after of the experiment realization. The difference between obtained values provides a feature of the stress levels subjected by the participant during the experiment. This level is measured in $\mu g/mL$. Instead of other features, these activations can suggest information about the increase or not of the long-term stress.

5

Stress Modeling

This chapter proposes a methodology to characterize reactions developing an experiment where stress is incited to a subject and his/her physiological signals are recorded. Once the system acquisition and the feature extraction are defined in previous chapters, next step is to create a stress model to approximate the Yerkes & Dodson curve. Data observations will be the features values and will be compared with the performance obtained for each experiment.

This thesis presents three experiments developed in controlled situations: 1) the first experiment consists on a subject playing neurocognitive games of increase difficulty mixed with relax periods, 2) the second proof shows the motorization of individuals while are discussing a public talk, and finally, 3) the third case is a complete system created to extract features and classify stress level in a five-start raking scale. This last experiment is a project founded for *AIRBUS* group

to classify stress levels of operator of Unmanned Aerial Vehicle (UAV) while are simulating a mission.

5.1 Stress Activations Playing Neurocognitive Games

Neurocognitive games have been recently introduced in our daily life with the evolution of the smart-phones technology. Who has not played *tetris* while being in the subway? or have escaped a stressful day playing five minutes before going to sleep?. But, do neurocognitive games really decrease our stress as their marketing says?. Which are the physiological features varying when we change our emotions?.

Emotional states could provoke changes in physiological signals and could be acquired to obtain information about the mental state of the individual. A first problem of this proposed supervised methods is that the time-line cannot be labeled to understand which is the subject state in each moment. Some authors have used neurocognitive games as ground truth to understand these human behaviors in a objective way. P. Renaud and J. Blondin [79] used *Stroop color* test [43], a recognition test with in congruent questions to obtain the individual performance based on number of correct answers. They concluded that a solid relation exists but this test does not overcome an individual characterization. E. Jovanov et al. [44] used specific military personal training to know the performance of a soldier based on time reaction to achieve a mission and correlated it with physiological responses, obtaining a high correlation, but was not rating in a scale to measure it.

This experiment is composed for an open scheme of neurocognitive games mixed with relaxing slots. The main objectives are:

- To determine relevant physiological features to estimate individual performance and compare with the scores obtained in each neurocognitive game.

- To classify between different states (relaxing or playing games) using only the most relevant features.

- To analyze the learning capabilities of a specific subject and show the differences between all participants.

- To compare between the subjective impression of each subject and the objective results of the physiological features extracted.

The overview of this experiment is divided into three main steps: first one is a feature extraction algorithm applied over the heart rhythm, Galvanic Skin Response (GSR) and hormone cortisol signals, obtaining relevant features. Secondly, the experiment design and a multi-classification stage used to determine the performance state. Finally, a individual learning criteria is applied to compare objective impressions versus the physiological results obtained.

5.1.1 Stress Feature Extraction

The following eight stress features discussed in chapter 4 have been extracted from each record: Heart rhythm features: SDNN, RMSSD, pNN50 and LF/HF ratio. Electrodermal activity: slope of the signal, driver area and number of sparse driver activations. Hormone analysis: salivary cortisol.

The duration of each experiment is 106 minutes. The time window for each feature value is 1 minute. These features attempts to model the relationship between variables $x_{8\times106}$ by fitting a linear regression model to the observer data (scores obtained) $s_{1\times106}$. LASSO (Least Absolute Shrinkage and Selection Operator) [96] algorithm assigns different weights $w_{1\times8}$ to each of the input variables depending on the information provided by each one.

The selection of the most relevant features is calculated using the Mean Square Error (MSE) between normalized scores and the linear regression obtained. $MSE_j = \sum_{i=1}^{N}(s_j - w_i x_i)^2$, where i is the iteration of the $i-th$ feature leave out of the MSE, N is the number of features and i is the subject. The MSE is calculated using the method Leave-One-Out (LOO) so this work find the minimum MSE obtained to know which features fit more in the linear regression.

5.1.2 Experiment Design

Classification between relaxing and playing games

The objective is to classify only using the most relevant features obtained in the previous subsection. We propose to perform a binary classification achieving the maximum accuracy using a cross validation. Different classification methods were tested: binary decision trees, regularized linear and quadratic discriminant analysis, naive Bayes model with Gaussian, k-nearest neighbors classification, support vector machine and random forest. Another problem proposed varies in a six multi-class support, where the same methods are used to classify between: relax time, speed, memory, attention, flexibility and problem solving tests.

Individual learning criteria

Subjects perform the experiment twice in order to know the capacity of learning the repetition of the same action one week later. A priori, scores should be higher the second time, since taking into account that the subject already knows the game and his ability to overcome himself. The technique to evaluate these scores is a simple ratio, where: $learning\ ratio_i = \overline{Score\ 2nd\ time_i}/\overline{Score\ 1st\ time_i}$, where i is the category game or relax time and $\overline{x}$ denote the mean average. Note the observed data $s_{1\times 106}$ is a interpolated linear regression of the scored obtained for each test.

Objective impression versus physiological subjectives results

The experiment consists of a set of neurocognitive tasks that measure five aspects: speed, memory, attention, flexibility and problem solving abilities. These tasks are developed by *Lumosity labs* and this experiment is composed by two games for each category (a total of ten games per experiment).

- Speed test: the intended primary skill targets are brain processing speed and participant reaction time.

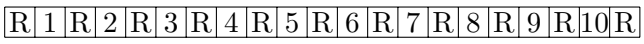

Figure 5.1: Experiment overview, where integer numbers represent the slot of each test and letter 'R', relax time. Note that number 1 and 6 belong speed tests, and so on: memory tests are 2 and 7, attention 3 and 8, flexibility 4 and 9, and problem solving tasks are 5 and 10.

- Memory tests: they are categorized under memory brain area, focusing on short-term memory.

- Attention tests: they are selective attention combined with multitasking.

- Flexibility tests: they are meant to determine mental skills to process multiple tasks simultaneously and the ability to switch between them.

- Problem solving tests: participants are expected to work through the details of a problem to reach a solution.

Finally, each participant fill a subjective questionnaire where they are asked what performance they think they have obtained from 1 to 5, where 1 was the worse and 5 the best performance. A multinomial logistic regression model was fit for each participant. The output was an integer number from 1 to 5, trying to compare these objective magnitudes with the subjective answers for each participant.

Relax time vs neurocognitive games

Experiment consists on an alternating set of games followed by a 150 seconds of participant relax. The hold time is 106 minutes. A representation of the schedule is shown in Fig. 5.1. It has been completed on a set of 24 participants with age interval from 20 to 59, mean age of the group was 29.16 years, with a standard deviation of 5.76. All subjects have undergone the experiment on a voluntary basis.

Data acquisition

Two non-intrusive sensors were used to measure physiological signals. The devices selected have been chosen from a wide range of available commercial sensors due to their reliability and small size.

Heart rhythm features acquired with *Microsoft Band 2* [71]: is a compact wristband that allows obtaining data about GSR, heart rate, Inter-Beat (RR) interval, device position and angular velocity.

Electrodermal activity recorded with *Q sensor* [1]. *Q sensor* allows the measurement of galvanic skin activity through two silver electrodes placed on the base of the sensor.

5.1.3 Results

Figure 5.2 shows an example of the GSR and Heart Rate (HR) signals recorded, and the scores obtained for one subject. The representations show results obtained for half experiment, where five test and each relax period are divided. Individual performance is simulated from different scores obtained on games with the given reaction time and to the correct answers of the tasks.

A Least Absolute Shrinkage and Selection Operator (LASSO) regression of the extracted features was fulfilled, using $\beta = 0.01$. Fig. 5.3 shows an example of how this regression adjust to the normalized scores, appearing rise during performed tasks and falls while rest periods.

Performing MSE function cost and the LOO method called before, the most relevant features that adjust better the regression was: (1) driver area of galvanic skin responses, and (2) LF/HF ratio and (3) Standard Deviation of NN Intervals (SDNN) of heart activity.

Classification results are shown in Table I, where appear the probability of error for each subject, between relax (Re) and games (Ga), and finally a the totals (T). This results were performed using the best accuracy option, a cross validation of

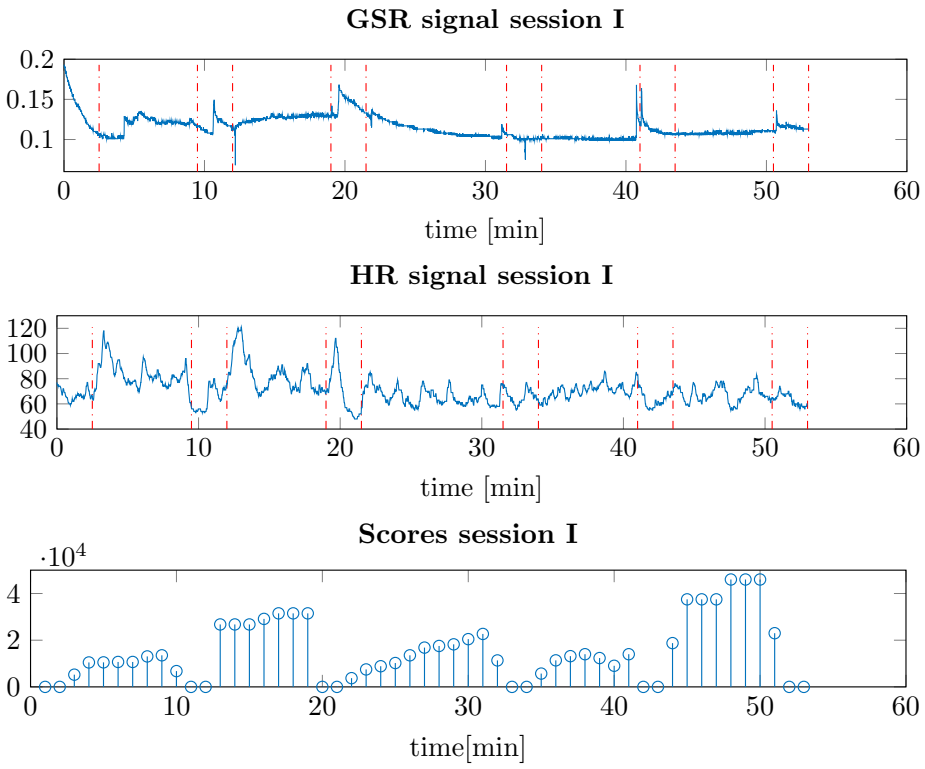

Figure 5.2: Example of data collected for half session of the experiment (53 minutes). Vertical red lines represent the differentiation between relax times and test. First subfigure (upper) shows GSR, Second (medium) the Heart Rate recorder and last figure (lower) the scores obtained.

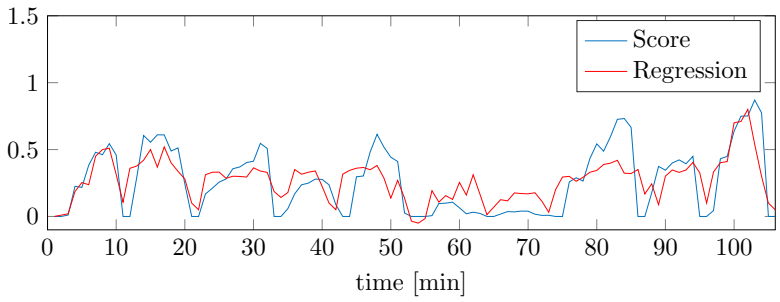

Figure 5.3: Example of a linear regression. Line blue represent the scores obtained for the participant (zero in relax times) and in color red the regression obtained using physiological signals.

Bayes naive with 64 neighbors and euclidean distance applied. Multi-classification was also calculated using a multi-modal logistic regression, optimizing the residual. In this case, as shown in Table I, it has higher errors differencing between games (g1, g2, g3, g4 and g5) and relax time (Re).

Learning averages are displayed in Table I, showing a statistical reporting for each subject. Finally, a rational quadratic regression was implemented to obtain an objective performance (Cl) and compare with the subjective (Qu) obtaining MSE between both.

#	(1) Relax vs games [Pe]			(2) Classification between games [Pe]							(3) Individual Learning averages [ratio]						(4) Comparative		
	Re	Ga	T	g1	g2	g3	g4	g5	Re	T	g1	g2	g3	g4	g5	T	Qu	Cl	MSE
1	30.77	6.25	12.26	75.00	62.50	87.50	43.75	50.00	53.85	61.32	1.22	1.31	1.45	1.34	1.88	1.44	4	1	9
2	23.08	7.50	11.32	50.00	50.00	62.50	81.25	50.00	57.69	58.49	0.45	0.32	0.80	0.70	1.10	0.67	2	3	1
3	23.08	7.50	11.32	50.00	81.25	56.25	37.50	75.00	42.31	55.66	1.20	1.34	1.34	1.56	2.23	1.53	4	4	0
4	30.77	10.00	15.09	43.75	18.75	31.25	62.50	43.75	96.15	53.77	1.60	1.22	1.76	1.22	4.20	2.00	5	5	0
5	30.77	6.25	12.26	93.75	75.00	56.25	68.75	62.50	50.00	66.04	2.02	0.43	0.65	0.54	5.30	1.79	4	3	1
6	26.92	7.50	12.26	50.00	50.00	50.00	75.00	43.75	57.69	54.72	1.30	0.45	0.43	0.98	1.11	0.85	3	3	0
7	38.46	8.75	16.04	75.00	75.00	93.75	43.75	56.25	42.31	62.26	2.51	1.22	1.23	1.03	1.00	1.40	3	4	1
8	19.23	7.50	10.38	50.00	93.75	31.25	50.00	81.25	76.92	65.09	2.01	1.56	1.92	1.09	1.09	1.42	5	4	1
9	38.46	11.25	17.92	75.00	31.25	50.00	81.25	62.50	42.31	55.66	1.29	1.40	1.91	1.34	1.20	1.43	3	3	0
T	29.06	8.06	13.31	62.50	59.72	57.64	60.42	58.33	57.69	59.22	1.51	1.03	1.28	1.09	2.47	1.48	3.67	3.33	1.44

Table 5.1: Statistical report for each subject(#): (1) probability of error of binary classification between relax and games. (2) probability of error of a multi-class classification. (3) ratio between first and second experiment. (4) Comparative between subjective appreciation and objective regression

5.1.4 Conclusions

LASSO regression algorithm combined with a cost function determines that the most relevant features were: driver area of electrodermal activity, LF/HF ratio and SDNN of cardiac activity. These three features are the most used in stress detection, and this work demonstrates that these can also be useful.

In this experiment, the binary classifier distinguish between play games and relax slots achieving a 13.31% probability of error. A multi-modal classifier performed more poorly, achieving only 59,22% mean square error where it is not possible to correlate the type of game with physiological features.

Moreover, results of nine subjects has been shown in Table I where each one has different capabilities. Besides, on average, they have achieved a 1.48 learning ratio so it can be said that each participant learned while playing, and achieved better results once the games were already familiar to them.

Depending on the game, the learning time was different of the game, capability of learning change, for example, problem solving task has a ratio of 2.47 on average instead of 1.03 in memory test.

Finally, a regression fit physiological features in a subjective way, and correlate with the subjective appreciation of each person, reaching only a 1.44 MSE on average, as shown in Table I. This mean that the appreciation of each volunteers seem to be what his physiological reactions mean.

5.1.5 Stress States Classification

How did you feel when you start a public talk? Heart rate increase fast, your corporal temperature increases or your skin starts to sweat if you are not use to speak in public. These affective symptoms that appear can suppose the appearance of stress [31].

Emotional symptoms provoke changes in different physiological signals that can be monitored to detect stress. D. Wu et al. [104] captured physiological responses: GSR, respiration, electroencephalogram and electrocardiogram for identification and classification into several stress levels. Another case was Zhai and Barreto

[107], who acquired different affective features: GSR, blood volume pressure and pupil diameter to differentiate states (relax or mental stress) in computers user. Speech also plays a role in detecting stress as can be depicted form [17] where stress is estimated using pitch and speech energy features and [74] where Log Frequency Power Coefficients (LFPC) are used to detect stress and emotion.

5.2 Stress Detection in Public Talks

The main scope of this experiment is to extract physiological features of monitoring subjects discussing public talks and classify their stress levels. A novel dataset composed of 17 subjects is presented where speech, electrodermal activity and heart rhythm were recorder using non-intrusive sensors. A proposed classifier determine the status of 8 volunteers of the dataset: [A] pre-presentation period, [B] talk, [C] questions. The differentiation between theses three classes are imposed to replicate the protocol used in Trier Social Stress Test (TSST) test. Another authors also used this three intervals to: show stress activations induced cortisol levels [103], stress detection from speech using Galvanic Skin Responses [46], or acute stress and its relation with chronic trapezius myalagia [93].

The following twelve stress features have been extracted from each record: Heart rhythm features: SDNN, RMSSD, pNN50, and LF/HF ratio. Electrodermal activity: slope of the signal, driver area, and number of sparse driver activations. Speech: estimated pitch, voicing probability, jitter, shimmer, and smoothed energy.

The feature vector can be denoted as $x_{12\times D}$, where D is the duration of the speech in minutes and 12 are the number of features. Several multi-class supervised classification methods were tested: k-nn neighborhoods, multi-class logistic regression and decision trees. Also non-supervised methods were validated as the expectation-maximization algorithm (EM) and Gaussian Mixture Models with Dirichlet Process (GMM-DP).

The models are trained using 9 talks as training set and tested in the rest. Note that monitoring each talks needs the acceptance of each individual, storage

all the data and process it which involves difficult to make bigger the database.

Finally, the algorithm proposed was an multi-class logistic classifier parametrized by a weight matrix and a bias vector (W,b). Mathematically can be formulated as:

$$P(Y = i|x, W, b) = \frac{e^{W_i x + b_i}}{\sum_1 e^{W_j x + b_j}}$$

, corresponding to each class (y_i) logistic classifier is characterized by a set of parameters (W_i,b_i).

5.2.1 Experimental Set-up

The experiment has been completed on a set of 17 participants with age interval from 20 to 59, mean age of the group was 27.21 years, with a standard deviation of 4.32. All subjects have undergone the experiment on a voluntary basis.

Three non-intrusive sensors were used to measure physiological signals. The devices selected have been chosen from a wide range of available commercial sensors due to their reliability and small size. The different signal are acquired using the following devices and configurations:

- **Heart rhythm signal** is acquired with *Microsoft Band 2* [71], it is a compact wristband that allows obtaining data about galvanic skin responses (GSR), heart rate, RR interval, device position and angular velocity.

- **Electrodermal activity** is recorded with a *Q sensor* [1]. It allows the measurement of galvanic skin activity through two silver electrodes placed on the base of the sensor.

- **Speech** is obtained using a Zoom H1 handheld recorder with a Rode lavalier microphone. Non lossy compressed files (wav), 24-bit quantification and 44 kHz sampling rate are used.

The captured signals and the computed features can be download form [35].

#	Classification between states				
	Duration (min)	A	B	C	Average
1	43	00.00	16.67	8.33	13.95
2	40	00.00	30.00	18.18	20.00
3	57	00.00	8.51	20.00	1.75
4	66	20.00	17.02	11.11	16.67
5	58	00.00	12.90	57.89	25.86
6	66	00.00	14.29	22.22	15.15
7	63	50.00	14.89	14.29	15.87
8	63	00.00	12.50	12.50	11.11
Average	57	15.85	8.06	20.57	15.05

Table 5.2: Statistical report for each subject(#): probability of error of a multi-class classification. Each column represent: (1) speaker identifier, (2) Duration of the talk, (3) Probability of error before talk [A], (4) Probability of error during talk [B], (5) Probability of error in question time [C] and (6) Total average.

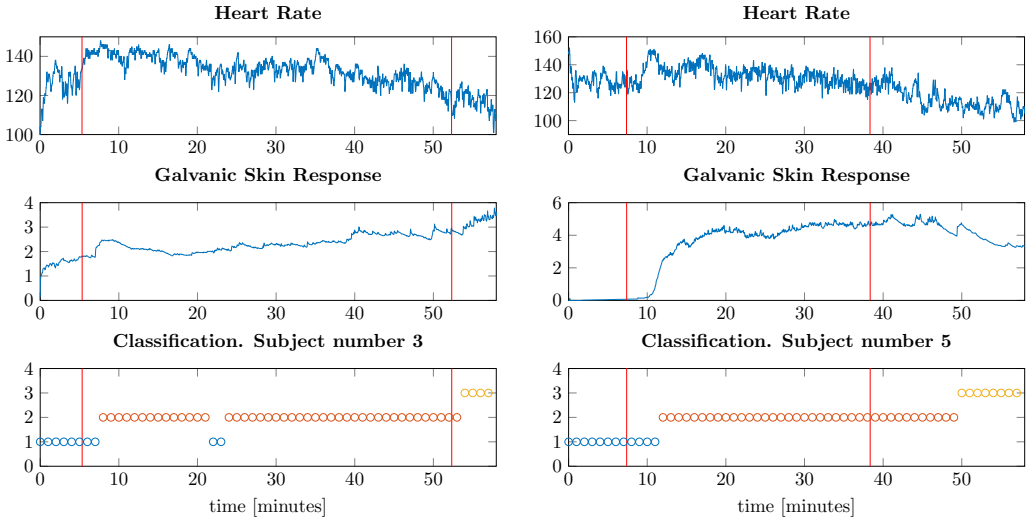

Figure 5.4: Examples of data classified of the experiment. Vertical red lines represent the differentiation between states: before talk [state A], talk [state B] and questions [state C]. Left figure corresponds to number 3 subject and right to number 5. First sub-figure (upper) shows Heart Rate, Second (medium) the Galvanic Skin Response and last figure (lower) the classification obtained in three classes: blue, red and yellow.

5.2.2 Results

Multi-class logistic regression algorithm achieves the better accuracy of the models raised before. Table 1 display the probability of error achieved for classification obtained. It is displayed the duration of the talks and the probability of error for each time division: probability of error pre-presentation period [A], probability of error during talk [B], probability of error in question time [C]. Besides an average column is included for further conclusions. Fig. 2 shows two examples of the heart rate, galvanic skin response and the classification obtained for the subjects number 4 and number five displayed in Table 5.2.

5.2.3 Conclusions

Model proposed was selected among many others used because obtain the best accuracy no over-fitting. Table 1 represents the multi-class classification obtained using a multi-class regression algorithm. Results show a 15.05% probability of error in average that confirms stress features were well chosen and model achieve the expectations.

Two examples of the recorded signals and their stress classification were displayed in Fig. 2 to understand the model proposed. The classifier also give the more relevant features (W): the slope of the GSR signal, the LF/HR ratio of heart rhythm and the estimated speech pitch.

5.3 Five-Levels Real-time Stress Classification

Daily work supposes the first factor of stress as it was mentioned in this thesis introduction [80]. In fact, depends on the type of work can be more dangerous, need a deal of concentration, questions of the boss could imply an extra difficulty, anxiety situations, etc. Therefore a wrong decision can bring serious consequences. Besides, also depends on the individual performance for each person: how reacts the worker in presence of pressure or indecision situations, and if s/he is trained and qualified to this end.

The aim of this experiment is to monitor a UAV operator in his/her work

environment and determine in real-time his/her stress level. These kind of workers are trained in pressure situations, so first the system should characterized each individual and them, test it in a real work environment situation. The operator use to be sitting but also use to move around the UAV controller so the system acquisition should acquire the signals in a non-intrusive way.

The hold system analyzes physiological signals captured and the output is a level of stress from one to five, where one seem the most relaxed and five the most stressed. Another additional outputs could be: no signal (NS) and died (D).

This work is subdivided in three parts: individual stress characterization for each operator, a complete real-time system for stress classification and some results and conclusions obtained.

5.3.1 Stress Characterization

Two operators of UAV were asked in voluntary basis to fulfill the neurocognitive games presented in Section 5.1.2. They completed the experiment twice, with a month of difference between them.

The games could be clustered in five abilities:memory, attention, speed, flexibility and problem solving tests. Figure 5.5 presents the difference between first and second sessions in average for each participant. As are scores normalized, the capacity of learning can be extracted for each participant and also know if they are over/under the global mean (normalized as 1).

Second question is to characterize the Yerkes & Dodson curve named in chapter 1 and can be found in Figure 1.1. Each test is normalized and of increased complexity. Also taking the average for all the tests, Figure 5.6 represents the mean average scores normalized by difficulty. These curves shows the level of difficulty from 1 to 9 and the y-axis represents the level of performance. Both representations show a similar inverted-U as the YerKes & Dodson curve.

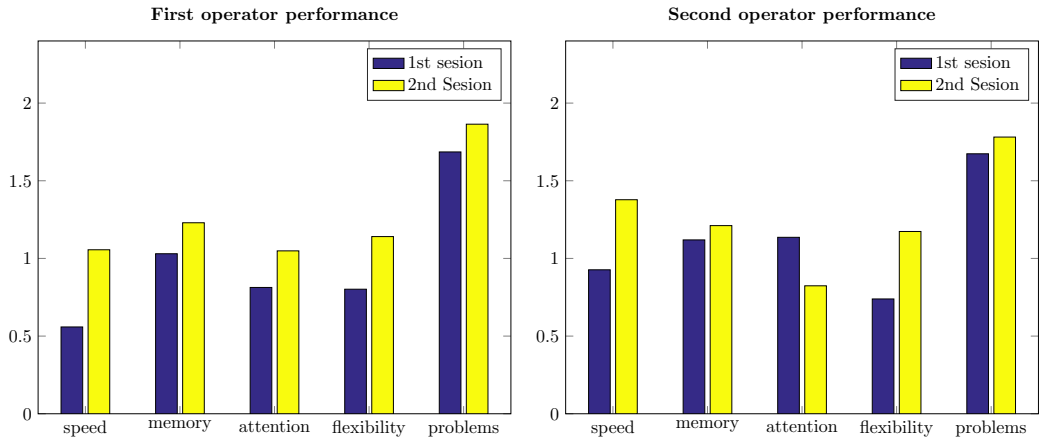

Figure 5.5: Comparative between the scores obtained in the first and second sessions.

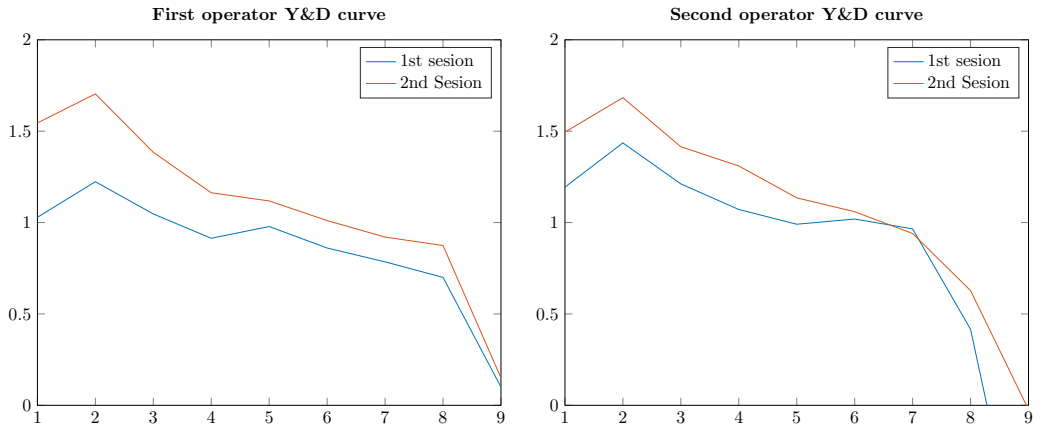

Figure 5.6: Simulated Yerkes & Dodson curves for each participant and session.

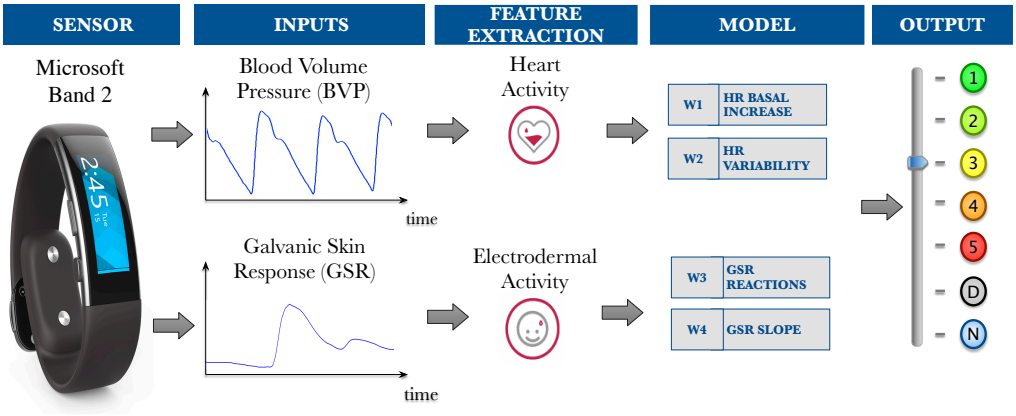

Figure 5.7: Graphical scheme of the real-time acquisition, signal processing and stress level classification.

5.3.2 System Set-up

A complete real-time system was developed for stress level assessment. The scheme of this system, that can be followed in Figure 5.7, is composed of:

- A non-intrusive sensor, Microsoft Band 2, that monitor heart rhythm and electrodermal activity signals, and send the values and their correspondent timestamps to a threat installed in a computer.
- A threat developed in *Visual Studio* is waiting each second for a package send from the sensor via *bluetooth*. Once it receive the values in form of package, the program save them in a buffer.
- Another threat in parallel send the package from *Visual Studio* to *Matlab*.
- *Matlab* receives each second a package and process it in frames of 60 seconds.
- The final output is a stress level assessment closed in a five-star rating scale.

5.3.3 Results

Two different reports are developed. The first one is real-time report of 60 seconds that display the Heart Rate and GSR signals and the correspondent level of stress. An example is displayed in Figure 5.8.

Figure 5.8: Example of real-time demonstrator report of 60 seconds.

The second report is an overview for an session finished. Figure 5.9 shows an example of an record of 15 minutes while an operator was working.

In general for every work session worked use to be at level 3 that implies that a normal performance. In some critical slot time the level of stress increases because of lot of warning or a critical problem. In the other hand, the levels could decrease from 3 if the UAV is totally controlled or stooped.

5.3.4 Conclusions

In this experiment two objectives have been achieved. First one is to characterize an individual because the reaction of each person are different even performing the same activity. This experiment presents a controlled test where the capacities for each volunteer in five different abilities: speed, memory, attention, flexibility and problem solving tests. Besides, Figure 5.5 is normalized to 1 where respect to a global average mean. An individual Yerkes & Dodson curve is also defined in term of the level difficulty that is shown in Figure 5.6.

On the other hand, a real-time classifier was implemented based on Heart Rate and Electrodermal activity. A *Microsoft Band 2* captured the signals and send it to a computer that analyze and decide the level of stress. This system is a

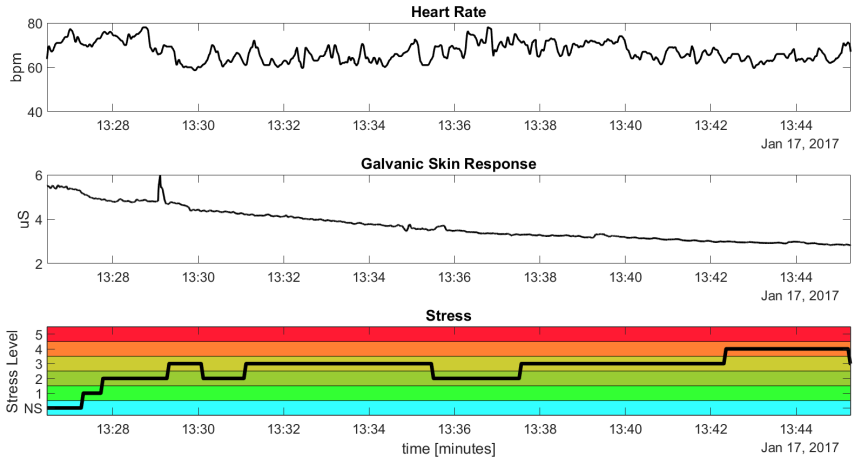

Figure 5.9: Example of a report of an experiment of 15 minutes.

complete real-time non-intrusive level assessment that cloud be useful to manage the workload for each operator. Basides, this method can be extrapolated to others critical workers, such as, comercial flight pilots, police, etc.

6

Conclusions

This thesis improves different aspects of stress evaluation previously proposed in the literature: we propose a new method of electrodermal reactions and jointly, we propose different physiological features to identify stress. Three experiments, in a controlled environment, have been developed to validate the global feature extraction and to obtain interpretable results by machine learning algorithms. The main conclusions of this work are summarized and some possible future lines are discussed.

6.1 Conclusions

The main results of the thesis are summarized below:

- A new feature extraction method for Galvanic Skin Response (GSR) signals

is presented. The method is faster than other benchmark techniques in the literature and can be implemented in a wearable sensor network. The contributions of this chapter were presented in [39].

- An exhaustive state-of-the art study about stress recognition has been presented.
- A complete stress feature extraction model is discussed including the cited algorithm [36] of GSR responses, and some common methods for heart rhythm, speech and cortisol hormone analysis.
- Three experiments are implemented to validate the feature extraction model proposed.
  - The first one captured signals and extract features in a controlled environment while the subject plays neurocognitive games. We obtain the most relevant features using a linear regression they are the: driver area of electrodermal activity, the LF/HF ratio and the Standard Deviation of NN Intervals (SDNN) of cardiac activity.
  - The second experiment is a controlled environment of public talks. It shows a percentage of 15.05% probability of error in average detecting different states such as between talk, before and after talks, by using the feature extraction model proposed in Chapter 4.
  - The last experiment applies the complete novel system that identifies the stress reaction employing the proposed techniques. The system captures in real-time physiological signals and classifies in a five levels rating scale.

6.2 Future Lines

This work also suggests several futures lines for further research in the stress modeling system with wearable sensors. We provide below a list with what we consider are some potential research lines.

Real-time stress bracelet. This thesis has overcome a feature extraction model for stress assessment and could be implemented in a wearable sensor. A proposed application of this method should be a linear classifier that notifies the level of stress in real-time. The bracelet should include a display showing a number normalized in a scale as a commercial wearable.

Workload assessment. In a work environment, it should be useful a non-intrusive system to know the level of stress, and to increment or decrement the workload in time. This technique can be implemented in critical works such as: operators of Unmanned Aerial Vehicle (UAV), polices, flight pilots, firefighters, etc, depending on the need.

References

[1] Affectiva. Qsensor. `http://qsensor-support.affectiva.com/`.

[2] Jordi Aguiló, Pau Ferrer-Salvans, Antonio García-Rozo, Antonio Armario, Ángel Corbí, Francisco J Cambra, Raquel Bailón, Ana González-Marcos, Gerardo Caja, Sira Aguiló, et al. Project ES3: Attempting to quantify and measure the level of stress. *Revista de neurologia*, 61(9):405–415, 2015.

[3] D. M. Alexander, C. Trengove, P. Johnston, T. Cooper, J. P. August, and E. Gordon. Separating individual skin conductance responses in a short interstimulus-interval paradigm. *Journal of Neuroscience Methods*, 146(1):116–123, 2005.

[4] Guillermo N Armaiz-Pena, Susan K Lutgendorf, Steve W Cole, and Anil K Sood. Neuroendocrine modulation of cancer progression. *Brain, behavior, and immunity*, 23(1):10–15, 2009.

[5] Armando Barreto and Jing Zhai. Physiologic Instrumentation for Real-time Monitoring of Affective State of Computer Users. *WSEAS Transactions on Circuits and Systems*, 3:496–501, 2003.

[6] Armando Barreto, Jing Zhai, and Malek Adjouadi. Non-intrusive physiological monitoring for automated stress detection in human-computer interaction. *Human–Computer Interaction*, pages 29–38, 2007.

[7] Mathias Benedek and Christian Kaernbach. A continuous measure of pha-

sic electrodermal activity. *Journal of Neuroscience Methods*, 190(1):80–91, 2010.

[8] Mathias Benedek and Christian Kaernbach. Decomposition of skin conductance data by means of nonnegative deconvolution. *Psychophysiology*, 47(4):647–658, 2010.

[9] Wolfram Boucsein. *Electrodermal activity*. Springer Science & Business Media, 2012.

[10] M M Bradley and P J Lang. Handbook of psychophysiology. *Handbook of psychophysiology*, 2000.

[11] Margaret M Bradley and Peter J Lang. Handbook of psychophysiology, 2007.

[12] Phillip J Brantley, Craig D Waggoner, Glenn N Jones, and Neil B Rappaport. A daily stress inventory: Development, reliability, and validity. *Journal of behavioral medicine*, 10(1):61–73, 1987.

[13] Monica F. Bugallo, Luca Martino, and Jukka Corander. Adaptive importance sampling in signal processing. *Digital Signal Processing*, 47(Supplement C):36 – 49, 2015.

[14] John T Cacioppo, Gary G Berntson, Jeff T Larsen, Kirsten M Poehlmann, Tiffany A Ito, et al. The psychophysiology of emotion. *Handbook of emotions*, 2:173–191, 2000.

[15] A. John Camm and Marek Malik. Heart rate variability. *European Heart Journal (1996)*, pages 354–381, 1996.

[16] Jongyoon Choi, Beena Ahmed, and Ricardo Gutierrez-osuna. Development and Evaluation of an Ambulatory Stress Monitor Based on Wearable Sensors. *Information Technology in Biomedicine, IEEE Transactions on,*, 16(2):279–286, 2012.

[17] L. Czap and J. M. Pintér. Intensity feature for speech stress detection. In *Proceedings of the 2015 16th International Carpathian Control Conference (ICCC)*, pages 91–94, May 2015.

[18] L. Martino D. Luengo. Almost rejectionless sampling from Nakagami-m distributions ($m \geq 1$). *IET Electronics Letters*, 48(24):1559–1561, 2012.

[19] Alain De Cheveigné and Hideki Kawahara. Yin, a fundamental frequency estimator for speech and music. *The Journal of the Acoustical Society of America*, 111(4):1917–1930, 2002.

[20] Bradley Efron, Trevor Hastie, Iain Johnstone, and Robert Tibshirani. Least angle regression. *The Annals of statistics - Institute of Mathematical Statistics*, 32(2):407–499, 2004.

[21] Michael Elad. Sparse and redundant representations: From theory to applications in signal and image processing, 2010.

[22] V. Elvira, L. Martino, D. Luengo, and M. F. Bugallo. Heretical multiple importance sampling. *IEEE Signal Processing Letters*, 23(10):1474–1478, 2016.

[23] Empatica. Empatica E4 wristband. `https://www.empatica.com/e4-wristband`.

[24] Florian Eyben, Felix Weninger, Florian Gross, and Björn Schuller. Recent developments in opensmile, the munich open-source multimedia feature extractor. In *Proceedings of the 21st ACM International Conference on Multimedia*, MM '13, pages 835–838, New York, NY, USA, 2013. ACM.

[25] Christos A Frantzidis, Evdokimos Konstantinidis, Costas Pappas, and Panagiotis D Bamidis. An automated system for processing electrodermal activity. *Studies in health technology and informatics*, 150:787, 2008.

[26] Hugues Garnier and Liuping Wang. *Identification of Continuous-time Models from Sampled Data*. Springer Science & Business Media, 2008.

[27] Alberto Greco, Gaetano Valenza, Antonio Lanata, Enzo Pasquale Scilingo, and Luca Citi. cvxeda: A convex optimization approach to electrodermal activity processing. *IEEE Transactions on Biomedical Engineering*, 63(4):797–804, 2016.

[28] John E Hall. *Guyton and Hall textbook of medical physiology*. Elsevier Health Sciences, 2010.

[29] Jennifer A Healey and Rosalind W Picard. Detecting stress during real-world driving tasks using physiological sensors. *IEEE Transactions on intelligent transportation systems*, 6(2):156–166, 2005.

[30] Jennifer A Healey and Rosalind W. Picard. Detecting stress during real-world driving tasks using physiological sensors. *Intelligent Transportation Systems, IEEE Transactions on*, 6(2):156–166, 2005.

[31] Javier Hernandez, Pablo Paredes, Asta Roseway, and Mary Czerwinski. Under Pressure: Sensing Stress of Computer Users. *Proceedings of the 32nd annual ACM conference on Human factors in computing systems - CHI '14*, pages 51–60, 2014.

[32] Javier Hernandez, Ivan Riobo, Agata Rozga, Gregory D Abowd, and Rosalind W Picard. Using electrodermal activity to recognize ease of engagement in children during social interactions. In *Proceedings of the 2014 ACM International Joint Conference on Pervasive and Ubiquitous Computing*, pages 307–317. ACM, 2014.

[33] Javier Hernandez Rivera. *Towards wearable stress measurement*. PhD thesis, Massachusetts Institute of Technology, 2015.

[34] Alberto Hernando, Jesús Lázaro, Eduardo Gil, Adriana Arza, Jorge Mario Garzón, Raúl López-Antón, Concepción de la Cámara, Pablo Laguna, Jordi Aguiló, and Raquel Bailón. Inclusion of respiratory frequency information in heart rate variability analysis for stress assessment. *IEEE journal of biomedical and health informatics*, 20(4):1016–1025, 2016.

[35] Hernando-Gallego and F. de la Calle Silos. Public talks stress dataset. http://www.tsc.uc3m.es/~fsilos/stress_dataset.zip.

[36] F. Hernando-Gallego. Sparse eda. https://github.com/fhernandogallego/sparsEDA.

[37] F. Hernando-Gallego and A. Artés-Rodríguez. Individual performance calibration using physiological stress signals. *Workshop on IEEE Conference on Body Sensor Networks (2015)*, July 2015.

[38] F. Hernando-Gallego and A. Artés-Rodríguez. Physiological Feature Extraction in Neurocognitive Games. *IEEE Conference on Body Sensor Networks (2018)*, Under revision 2017.

[39] F. Hernando-Gallego, D. Luengo, and A. Artés-Rodríguez. Feature Extraction of Galvanic Skin Responses by Non-Negative Sparse Deconvolution. *IEEE Journal of Boimedical and Health Informatics*, pages 1–1, 2017.

[40] F. Hernando-Gallego, F. Silos, and A. Artés-Rodríguez. Stress States Classification Using Physiological Signals During Public Talks. *Acoustics, Speech, and Signal Processing (ICASSP) (2018)*, Under revision 2017.

[41] Eva Hudlicka. To feel or not to feel: The role of affect in human–computer interaction. *International journal of human-computer studies*, 59(1):1–32, 2003.

[42] Swayambhoo Jain, Urvashi Oswal, Kevin Shuai Xu, Brian Eriksson, and Jarvis Haupt. A compressed sensing based decomposition of electrodermal activity signals. *IEEE Transactions on Biomedical Engineering*, 64(9):2142–2151, 2017.

[43] Arthur R Jensen and William D Rohwer. The Stroop color-word test: A review. *Acta psychologica*, 25:36–93, 1966.

[44] Emil Jovanov, Amanda O. Lords, Dejan Raskovic, Paul G. Cox, Reza Adhami, and Frank Andrasik. Stress monitoring using a distributed wireless

intelligent sensor system. *Engineering in Medicine and Biology Magazine*, 22(3)(June):49–55, 2003.

[45] Clemens Kirschbaum, K-M Pirke, and Dirk H. Hellhammer. The 'Trier Social Stress Test'–a tool for investigating psychobiological stress responses in a laboratory setting. *Neuropsychobiology*, 28:76–81, 1993.

[46] Hindra Kurniawan, Alexandr V. Maslov, and Mykola Pechenizkiy. Stress detection from speech and Galvanic Skin Response signals. *Proceedings of the 26th IEEE International Symposium on Computer-Based Medical Systems*, pages 209–214, jun 2013.

[47] Sungjun Kwon, Jeongsu Lee, Gih Sung Chung, and Kwang Suk Park. Validation of heart rate extraction through an iphone accelerometer. In *Engineering in Medicine and Biology Society, EMBC, 2011 Annual International Conference of the IEEE*, pages 5260–5263. IEEE, 2011.

[48] Ledalab, University of Graz (Austria). GSR signal example. `http://ledalab.de/download/ivn07_16_matlab.mat`.

[49] Chong L. Lim, Chris Rennie, Robert J. Barry, Homayoun Bahramali, Ilario Lazzaro, Barry Manor, and Evian Gordon. Decomposing skin conductance into tonic and phasic components. *International Journal of Psychophysiology*, 25(2):97–109, feb 1997.

[50] David Luengo, Sandra Monzón, Tom Trigano, Javier Vía, and Antonio Artés-Rodríguez. Blind analysis of atrial fibrillation electrograms: a sparsity-aware formulation. *Integrated Computer-Aided Engineering*, 22(1):71–85, 2015.

[51] David Luengo, Javier Vía, Sandra Monzón, Tom Trigano, and Antonio Artés-Rodríguez. Cross-products LASSO. In *2013 IEEE International Conference on Acoustics, Speech and Signal Processing (ICASSP)*, pages 6118–6122, 2013.

[52] V G Macefield, B G Wallin, and a B Vallbo. The discharge behaviour of single vasoconstrictor motoneurones in human muscle nerves. *The Journal of physiology*, 481 Pt 3:799–809, 1994.

[53] Vaughan G Macefield and B Gunnar Wallin. The discharge behaviour of single sympathetic neurones supplying human sweat glands. *Journal of the autonomic nervous system*, 61(3):277–286, 1996.

[54] Gloria Mark, Shamsi Iqbal, Mary Czerwinski, and Paul Johns. Capturing the mood: facebook and face-to-face encounters in the workplace. In *Proceedings of the 17th ACM conference on Computer supported cooperative work & social computing*, pages 1082–1094. ACM, 2014.

[55] Andrea H. Marques, Marni N. Silverman, and Esther M. Sternberg. Evaluation of stress systems by applying noninvasive methodologies: Measurements of neuroimmune biomarkers in the sweat, heart rate variability and salivary cortisol. *NeuroImmunoModulation*, 17(3):205–208, 2010.

[56] L. Martino. Parsimonious adaptive rejection sampling. *Electronics Letters*, 53(16):1115–1117, 2017.

[57] L. Martino and J. Miguez and. A novel rejection sampling scheme for posterior probability distributions. *IEEE International Conference on Acoustics, Speech, and Signal Processing (ICASSP)*, 2009.

[58] L. Martino, R. Casarin, and D. Luengo. Sticky proposal densities for adaptive MCMC methods. *IEEE Workshop on Statistical Signal Processing (SSP)*, 2016.

[59] L. Martino, V. Elvira, D. Luengo, and J. Corander. An adaptive population importance sampler: Learning from uncertainty. *IEEE Transactions on Signal Processing*, 63(16):4422–4437, Aug 2015.

[60] L. Martino, V. Elvira, D. Luengo, and J. Corander. Layered adaptive importance sampling. *Statistics and Computing*, 27(3):599–623, 2017.

[61] L. Martino, V. Elvira, D. Luengo, J. Corander, and F. Louzada. Orthogonal parallel MCMC methods for sampling and optimization. *Digital Signal Processing*, 58(Supplement C):64 – 84, 2016.

[62] L. Martino and J. Míguez. Generalized rejection sampling schemes and applications in signal processing. *Signal Processing*, 90(11):2981–2995, November 2010.

[63] L. Martino, J. Read, and D. Luengo. Independent doubly adaptive rejection Metropolis sampling. *IEEE International Conference on Acoustics, Speech, and Signal Processing (ICASSP)*, 2014.

[64] L. Martino, J. Read, and D. Luengo. Independent doubly adaptive rejection Metropolis sampling within Gibbs sampling. *IEEE Transactions on Signal Processing*, 63(12):3123–3138, June 2015.

[65] L. Martino, H. Yang, D. Luengo, J. Kanniainen, and J. Corander. A fast universal self-tuned sampler within Gibbs sampling. *Digital Signal Processing*, 47:68 – 83, 2015.

[66] Luca Martino. A review of multiple try MCMC algorithms for signal processing. *Digital Signal Processing*, 75:134 – 152, 2018.

[67] Luca Martino, Victor Elvira, and Gustau Camps-Valls. The recycling Gibbs sampler for efficient learning. *Digital Signal Processing*, 74:1–13, 2017.

[68] Gerald Matthews, D Roy Davies, Rob B Stammers, and Steve J Westerman. *Human performance: Cognition, stress and individual differences*. Psychology Press, Philadelphia, 2000.

[69] Bruce S McEwen and Teresa Seeman. Stress and affect: Applicability of the concepts of allostasis and allostatic load. 2003.

[70] Medicom MTD Ltd. Medical equipment for neurophysiology, polysomnography, biofeedback and research. `http://www.medicom-mtd.com/en/`.

[71] Microsoft. Microsoft band 2. https://www.microsoft.com/microsoft-band/.

[72] Sandra Monzón, Tom Trigano, David Luengo, and Antonio Artés-Rodríguez. Sparse spectral analysis of atrial fibrillation electrograms. In *2012 IEEE International Workshop on Machine Learning for Signal Processing (MLSP)*, pages 1–6, 2012.

[73] Paul Jarle Mork and Rolf H Westgaard. The influence of body posture, arm movement, and work stress on trapezius activity during computer work. *European journal of applied physiology*, 101(4):445–56, nov 2007.

[74] T. L. Nwe, S. W. Foo, and L. C. De Silva. Detection of stress and emotion in speech using traditional and fft based log energy features. In *Fourth International Conference on Information, Communications and Signal Processing, 2003 and the Fourth Pacific Rim Conference on Multimedia. Proceedings of the 2003 Joint*, volume 3, pages 1619–1623 vol.3, Dec 2003.

[75] Juha Pärkkä, Juho Merilahti, Elina M Mattila, Esko Malm, Kari Antila, Martti T Tuomisto, Ari Viljam Saarinen, Mark van Gils, and Ilkka Korhonen. Relationship of psychological and physiological variables in long-term self-monitored data during work ability rehabilitation program. *IEEE Transactions on Information Technology in Biomedicine*, 13(2):141–151, 2009.

[76] DH Phan, S Bonnet, R Guillemaud, E Castelli, and NY Pham Thi. Estimation of respiratory waveform and heart rate using an accelerometer. In *Engineering in Medicine and Biology Society, 2008. EMBS 2008. 30th Annual International Conference of the IEEE*, pages 4916–4919. IEEE, 2008.

[77] Rosalind W Picard and Roalind Picard. *Affective computing*, volume 252. MIT press Cambridge, 1997.

[78] Miguel RAMOS, C Rovira, L Umfuhrer, and E Urbina. Sistema nervioso autónomo. revisión. *Revista de Posgrado de la Cátedra VIa Medicina*, 1(101), 2001.

[79] Patrice Renaud and JP Blondin. The stress of Stroop performance: physiological and emotional responses Renaud, P., & Blondin, J. (1997). The stress of Stroop performance: physiological and emotional responses to color-word interference, task pacing, and pacing speed. International Jour. *International Journal of Psychophysiology*, pages 87–97, 1997.

[80] Paul J Rosch. The quandary of job stress compensation. *Health and Stress*, 3(1):1–4, 2001.

[81] Evan Russell, Gideon Koren, Michael Rieder, and Stan Van Uum. Hair cortisol as a biological marker of chronic stress: current status, future directions and unanswered questions. *Psychoneuroendocrinology*, 37(5):589–601, may 2012.

[82] Ioana Safta, Ovidiu Grigore, and Constantin Căruntu. Emotion detection using psycho-physiological signal processing. In *Advanced Topics in Electrical Engineering (ATEE), 2011 7th International Symposium on*, pages 1–4. IEEE, 2011.

[83] Björn Schuller, Stefan Steidl, and Anton Batliner. A.: The interspeech 2009 emotion challenge. In *In ISCA, ed.: Proceedings of Interspeech*, pages 312–315, 2009.

[84] Björn Schuller, Stefan Steidl, Anton Batliner, Felix Burkhardt, Laurence Devillers, Christian Müller, and Shrikanth Narayanan. The interspeech 2010 paralinguistic challenge. In *In Proc. Interspeech*, 2010.

[85] Cornelia Setz, Bert Arnrich, Johannes Schumm, Roberto La Marca, Gerhard Tröster, and Ulrike Ehlert. Discriminating stress from cognitive load using a wearable eda device. *IEEE Transactions on information technology in biomedicine*, 14(2):410–417, 2010.

[86] Yuan Shi, Minh Hoai Nguyen, Patrick Blitz, Brian French, Scott Fisk, Fernando De la Torre, Asim Smailagic, Daniel P Siewiorek, Mustafa al'Absi,

Emre Ertin, et al. Personalized stress detection from physiological measurements. In *International symposium on quality of life technology*, pages 28–29, 2010.

[87] Shimmer. *ExG User Guide for ECG*. www.shimmersensing.com, Realtime Technologies Ltd, 2014.

[88] Shimmer. *ExG User Guide for EMG*. www.shimmersensing.com, Realtime Technologies Ltd, 2014.

[89] Shimmer. *GSR + Expansion Board User Guide*. www.shimmersensing.com, Realtime Technologies Ltd, 2014.

[90] Shimmer. *Optical Pulse Sensing Probe User Guide*. www.shimmersensing.com, Realtime Technologies Ltd, 2014.

[91] Shimmer Sensing. Shimmer 3 GSR unit. `http://www.shimmersensing.com/products/shimmer3-wireless-gsr-sensor`.

[92] Mandeep Singh and AB Queyam. Stress Detection in Automobile Drivers using Physiological Parameters: A Review. *International Journal of Electronics Engineering*, 5(2):1–5, 2013.

[93] Anna Sjörs, Britt Larsson, Björn Karlson, Kai Osterberg, Joakim Dahlman, and Björn Gerdle. Salivary cortisol response to acute stress and its relation to psychological factors in women with chronic trapezius myalgia. *Psychoneuroendocrinology*, 35(5):674–85, jun 2010.

[94] Sara Taylor, Natasha Jaques, Weixuan Chen, Szymon Fedor, Akane Sano, and Rosalind Picard. Automatic Identification of Artifacts in Electrodermal Activity Data. *Engineering in Medicine and Biology Society (EMBC), 2015 37th Annual International Conference of the IEEE*, pages 1934–1937, 2015.

[95] João Paulo Teixeira and André Gonçalves. Accuracy of jitter and shimmer measurements. *Procedia Technology*, 16:1190 – 1199, 2014.

[96] Robert Tibshirani. Regression shrinkage and selection via the lasso. *Journal of the Royal Statistical Society. Series B (Methodological)*, pages 267–288, 1996.

[97] Chadi Touma, Rupert Palme, and Norbert Sachser. Analyzing corticosterone metabolites in fecal samples of mice: a noninvasive technique to monitor stress hormones. *Hormones and Behavior*, 45(1):10–22, jan 2004.

[98] K Vedhara, J Hyde, I.D Gilchrist, M Tytherleigh, and S Plummer. Acute stress, memory, attention and cortisol. *Psychoneuroendocrinology*, 25(6):535–549, aug 2000.

[99] B Gunnar Wallin. Sympathetic nerve activity underlying electrodermal and cardiovascular reactions in man. *Psychophysiology*, 18(4):470–476, 1981.

[100] Duolao Wang, Yin Bun Cheung, Radivoj Arezina, Jorg Taubel, and Alan John Camm. A nonparametric approach to qt interval correction for heart rate. *Journal of biopharmaceutical statistics*, 20(3):508–522, 2010.

[101] Quan Wang. COSBOS: COlor-Sensor-Based Occupancy Sensing. `https://se.mathworks.com/matlabcentral/fileexchange/48428-cosbos--color-sensor-based-occupancy-sensing/content/COSBOS_v1.0/LTM_Recovery/Lib/SparseLab2.1-Core/Solvers/SolveLasso.m`, 12 Nov. 2014.

[102] Elliot D Weitzman, David Fukushima, Christopher Nogeire, Howard Roffwarg, T F Gallagher, and Leon Hellman. Twenty-four hour pattern of the episodic secretion of cortisol in normal subjects. *The Journal of Clinical Endocrinology \& Metabolism*, 33(1):14–22, 1971.

[103] Oliver T. Wolf, Nicole C. Schommer, Dirk H. Hellhammer, Bruce S. McEwen, and Clemens Kirschbaum. The relationship between stress induced cortisol levels and memory differs between men and women. *Psychoneuroendocrinology*, 26(7):711–720, oct 2001.

[104] Dongrui Wu, Christopher G. Courtney, Brent J. Lance, Shrikanth S. Narayanan, Michael E. Dawson, Kelvin S. Oie, and Thomas D. Parsons. Optimal Arousal Identification and Classification for Affective Computing Using Physiological Signals: Virtual Reality Stroop Task. *IEEE Transactions on Affective Computing*, 1(2):109–118, jul 2010.

[105] Robert M Yerkes and John D Dodson. The relation of strength of stimulus to rapidity of habit-formation. *Journal of comparative neurology and psychology*, 18(5):459–482, 1908.

[106] Jing Zhai and Armando Barreto. Stress detection in computer users based on digital signal processing of noninvasive physiological variables. In *Engineering in Medicine and Biology Society, 2006. EMBS'06. 28th Annual International Conference of the IEEE*, pages 1355–1358. IEEE, 2006.

[107] Jing Zhai, Armando Barreto, Craig Chin, and Chao Li. Realization of stress detection using psychophysiological signals for improvement of human-computer interactions. *SoutheastCon , 2005. Proceedings. IEEE*, pages 415–420, 2005.

[108] Philippe Zimmermann, Sissel Guttormsen, Brigitta Danuser, and Patrick Gomez. Affective computing—a rationale for measuring mood with mouse and keyboard. *International journal of occupational safety and ergonomics*, 9(4):539–551, 2003.